Journal of Medicinal Chemistry

Article

1,4-Substituted Triazoles as Non-Steroidal Antiandrogens for Prostate Cancer Treatment

Claudia Ferroni, Antonella Pepe, Yeong Sang Kim, Sunmin Lee, Andrea Guerrini, Marco Daniele Parenti, Anna Tesei, Alice Zamagni, Michela Cortesi, Nadia Zaffaroni, Michelandrea De Cesare, Giovanni Luca Beretta, Jane B. Trepel, Sanjay V. Malhotra, and Greta Varchi

J. Med. Chem., **Just Accepted Manuscript** • DOI: 10.1021/acs.jmedchem.7b00105 • Publication Date (Web): 08 Mar 2017

ACS Publications

Journal of Medicinal Chemistry is published by the American Chemical Society. 1155 Sixteenth Street N.W., Washington, DC 20036

1,4-Substituted Triazoles as Non-Steroidal Antiandrogens for Prostate Cancer Treatment

Claudia Ferroni,[¶][¥] Antonella Pepe,[‡¥] Yeong Sang Kim,[#] Sunmin Lee,[#] Andrea Guerrini,[¶] Marco Daniele Parenti,[¶] Anna Tesei,[§] Alice Zamagni,[§] Michela Cortesi,[§] Nadia Zaffaroni,[†] Michelandrea De Cesare,[†] Giovanni Luca Beretta,[†] Jane B. Trepel,[#] Sanjay V. Malhotra[∫] and Greta Varchi[¶]**

[¶]Italian National Research Council, Institute for the Organic Synthesis and Photoreactivity Via Gobetti 101 - 40129 Bologna, Italy

[‡]Purdue Center for Cancer Research, 720 Clinic Drive, West Lafayette, Indiana 47907, United States

[#]Center for Cancer Research, National Cancer Institute, National Institutes of Health, Building 10 - Magnuson CC, Bethesda, Maryland 20892, United States

[§]Biosciences Laboratory, Istituto Scientifico Romagnolo per lo Studio e la Cura dei Tumori (IRST), IRCCS, Via P. Maroncelli, 40 - 47014 Meldola, Forlì, Italy

[†]Fondazione IRCCS Istituto Tumori Milano, Via Amadeo, 42 - 20133 Milano, Italy

[∫]Department of Radiation Oncology, Division of Radiation and Cancer Biology, Stanford University School of Medicine, CA 94304, United States

[¥]These authors equally contributed to this work.

KEYWORDS prostate cancer, bicalutamide, enzalutamide, antiandrogens, triazole, click-chemistry.

ABSTRACT

Prostate cancer (PC) is the fifth leading cause of cancer death in men and the androgen receptor (AR) represents the primary target for PC treatment, even though the disease frequently progresses toward androgen-independent forms. Most of the commercially available non-steroidal antiandrogens show a common scaffold consisting of two aromatic rings connected by a linear or a cyclic spacer. By taking advantage of a facile, one-pot click chemistry reaction, we report herein the preparation of a small library of novel 1,4-substituted triazoles with AR antagonistic activity. Biological and theoretical evaluation demonstrated that the introduction of the triazole core in the scaffold of non-steroidal antiandrogens allowed the development of small molecules with improved overall AR-antagonist activity. In fact, compound **14d** displayed promising *in vitro* antitumor activity toward three different prostate cancer cell lines and was able to induce 60% tumor growth inhibition of the CW22Rv1 *in vivo* xenograft model. These results represent a step towards the development of novel and improved AR antagonists.

1. Introduction

Prostate cancer (PC) is the second most frequently diagnosed cancer and the fifth leading cause of death from malignancy in men worldwide.[1] The activation of the androgen receptor (AR) signaling has a pivotal role for PC development, progression and androgen-independent growth.[2,3]

AR belongs to the nuclear receptor family of transcription factors that mediates androgen action in cells upon ligand binding. The AR is widely distributed and is composed of a N-terminal transcriptional activation domain, a central DNA-binding domain, a short-hinge region, and a C-terminal ligand-binding domain (LBD), comprising a 12 helical structure.[3]

Endocrine therapy has been used in order to reduce androgen synthesis or block AR activation. So far, androgen-deprivation therapy (ADT) or treatment with first-generation antiandrogens represents the mainstay of treatment for advanced PC. However, most patients acquire resistance to long term treatment, thus developing more aggressive androgen-independent (AIPC) or castration-resistant (CRPC, formerly known as hormone-refractory prostate cancer) tumors.[4] In the past decades, research has proved that signaling through the AR continues to be fundamental for tumor growth despite castration.[5] Indeed, AR aberrations, including gene amplifications,[6] point mutations[7–9] as well as constitutively active splice variants, are implicated in CRPC.[2,10]

Antiandrogens are classified into steroidal and non-steroidal compounds. Steroidal anti-androgens were first developed in the late 1960s. Among these, cyproterone acetate (**1**, Fig. 1) acts by blocking the interaction of testosterone (T) and/or dihydrotestosterone (DHT) with the AR. Despite its effectiveness, cyproterone suffers from central and progestational side effects, namely impotence and loss of libido.[11]

First generation non-steroidal AR antagonists, such as flutamide, **2**,[12] hydroxyflutamide, **3**, bicalutamide, **4**, [13] and nilutamide, **5**, diminish androgenic effects by competitively inhibiting androgen-AR binding. However, after a short time of treatment (2 years), these antiandrogens may become partial AR agonists due to the occurrence of LBD point mutations and to the expression of active AR splice variants.[14] Therefore, improved understanding of the mechanisms underpinning resistance has led to the development of a second generation of steroidal or non-steroidal AR targeting molecules that significantly contribute to prolonging patient survival, such as abiraterone, **6**,[10] enzalutamide, **7** (formerly known as MDV3100)[15,16] and 4-(7-(4-cyano-3-(trifluoromethyl)phenyl)-8-oxo-6-thioxo-5,7-diazaspiro[3.4]octan-5-yl)-2-fluoro-*N*-methylbenzamide, **8** (ARN-509**)**.[17] Abiraterone was the first-in-class potent and selective CYP17 inhibitor that causes a decrease in adrenal androgens, thus inhibiting the AR signaling pathway by blocking ligand synthesis. Despite initial responses, several patients develop resistance within a year.[18] Enzalutamide and **8** are second-generation non-steroidal antiandrogens with high affinity binding for the AR LBD. In particular, enzalutamide received FDA approval in 2012 for the treatment of patients with metastatic castration-resistant PC who have previously received docetaxel.[19] However, a F876L missense mutation in the AR LBD has been shown to confer resistance to enzalutamide and **8**, by switching their activity on AR from antagonist to agonist.[20,21] Recently, Moilanen and coworkers described the discovery and the preclinical development of ODM-201, **9**,[22] a novel full antagonist for the mutant AR that demonstrated antitumor activity *in vitro* and *in vivo*.[23] Furthermore, Purushottamachar demonstrated that a phase 3 clinical agent, galeterone **10**, and its analogues are able to disrupt AR signaling through enhanced AR degradation.[24]

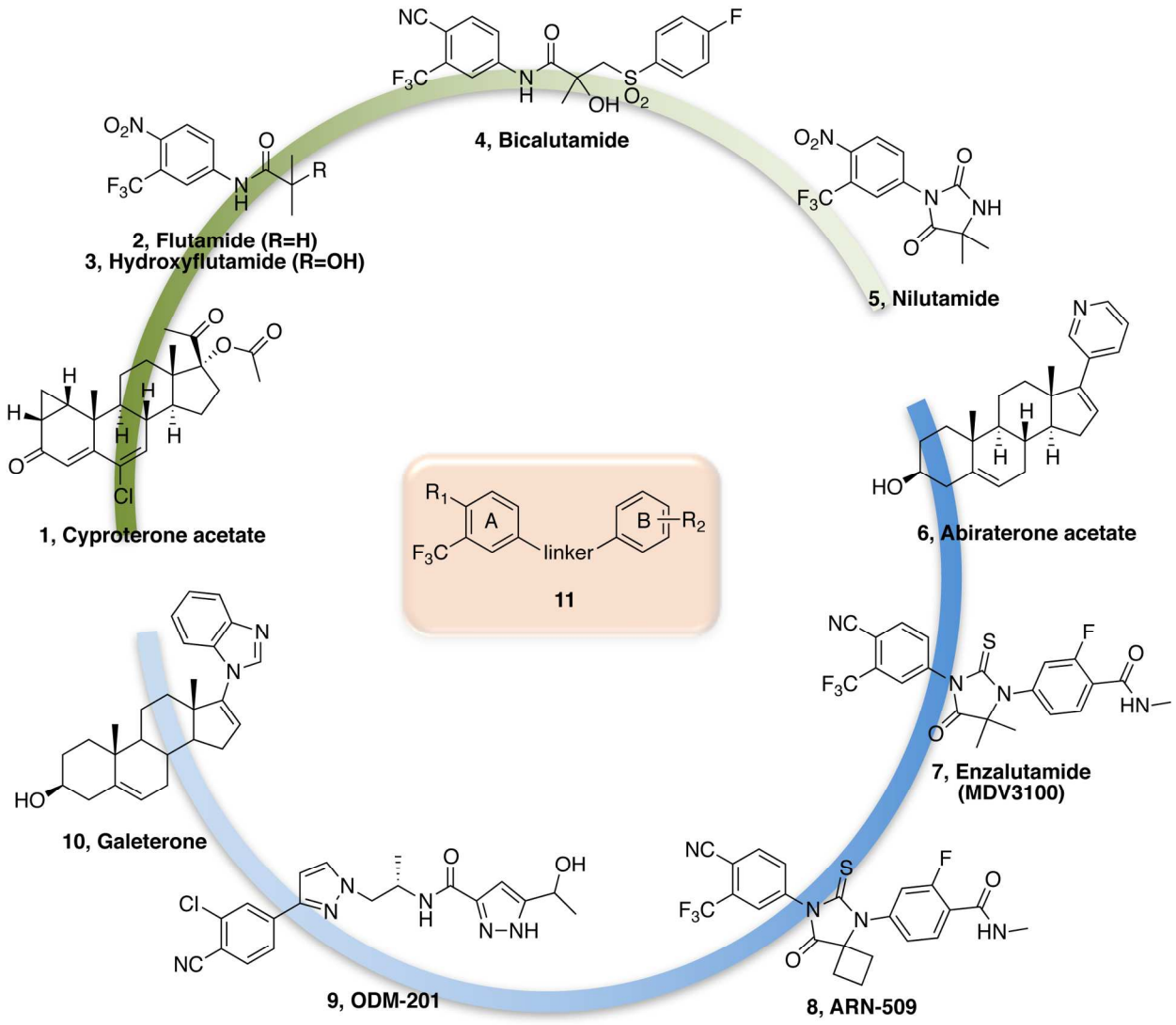

Figure 1. Androgen receptor targeting therapeutics for the treatment of PC.

Based on these findings, it is evident that the development of novel antiandrogens aimed at circumventing the mutation-based resistance of PC is an urgent need.[25] Commercially available non-steroidal antiandrogens show a common scaffold composed of two aromatic rings linked by a linear or a cyclic spacer (**11**, Fig. 1).

Searching for novel non-steroidal antiandrogen molecules,[26–29] we have discovered a new class of AR modulators bearing the triazole core. Triazoles are heterocyclic compounds that are often embedded in more complex molecules with important biological activity,[30] including

antibacterial, antifungal, anti-inflammatory, anti-HIV and recently as potential androgen receptor antagonists.[31] Triazole derivatives have been extensively used as amide bond isosteres, with the ability to increase molecule bioavailability and water solubility, and favor hydrogen bonding as well as dipole-dipole and π-stacking interactions. Furthermore, the 1,2,3-triazole core is extremely stable towards hydrolysis, oxidative/reductive conditions and metabolic degradation.[32]

Herein we report the preparation of a diverse library of 1,4-substituted triazoles able to reduce the level of prostate-specific antigen (PSA) and showing activity against a panel of prostate cancer cell lines, e.g. LNCaP, LNCaP-AR and CW22Rv1. Based on structure−activity relationship (SAR) study, we identified a promising hit molecule that was further tested *in vivo*.

2. Results and Discussion

2.1. Chemistry

The impressive advances in the "click" chemistry field along with the promising biological activity of 1,2,3-triazole derivatives, make them attractive targets in synthetic organic chemistry.[30] In order to obtain a large library of compounds, we performed the Huisgen 1,3-dipolar cycloaddition[33] between an azide moiety and a terminal alkyne. In particular, we used copper (I) catalyst (copper-alkyne-azide-cycloaddition, CuAAC) that dramatically accelerates the reaction rate, while making it highly regioselective and leading exclusively to the 1,4-disubstituted isomer.[34] CuAAC allowed to obtain the corresponding triazoles in high yield with a one-pot procedure starting from the aromatic amine and without azide isolation or purification.[35]

We synthesized substituted triazoles bearing none, one or two spacers between the aromatic rings and the triazole core (**I**, **II**, **III**; Fig. 2).

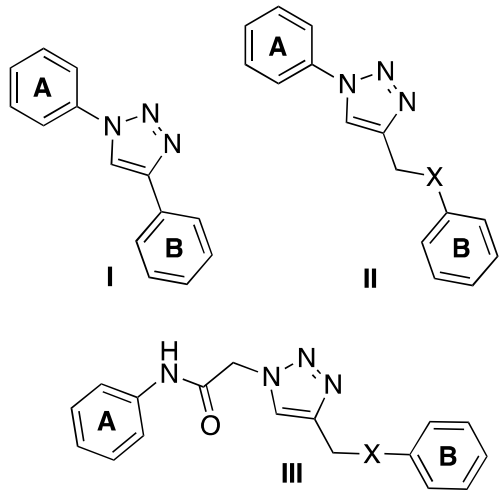

Figure 2. Classes of synthesized triazole derivatives.

Scheme 1 outlines the synthesis of derivatives of type **I**. Starting from commercially available aldehydes, the terminal alkynes (**2a**-**c**) were obtained through the Corey-Fuchs reaction;[36] aldehydes were easily converted to the corresponding di-bromo olefins (**1a**-**c**), which were then treated with lithium diisopropylamide (LDA) to afford the desired alkynes in good yields. Subsequently, 4-cyano-3-(trifluoromethyl)aniline was treated with *tert*-butyl nitrite (*t*-BuONO) and azidotrimethylsilane ($TMSN_3$) to generate the corresponding azide *in situ*. After 2 hours at 0°C, a catalytic amount of $CuSO_4$, sodium ascorbate, as reducing agent, and the terminal alkyne were added to the reaction mixture to afford the triazole derivatives (**3a**-**c**).

Scheme 1. Synthesis of no-spacer triazoles **3a-c**.[a]

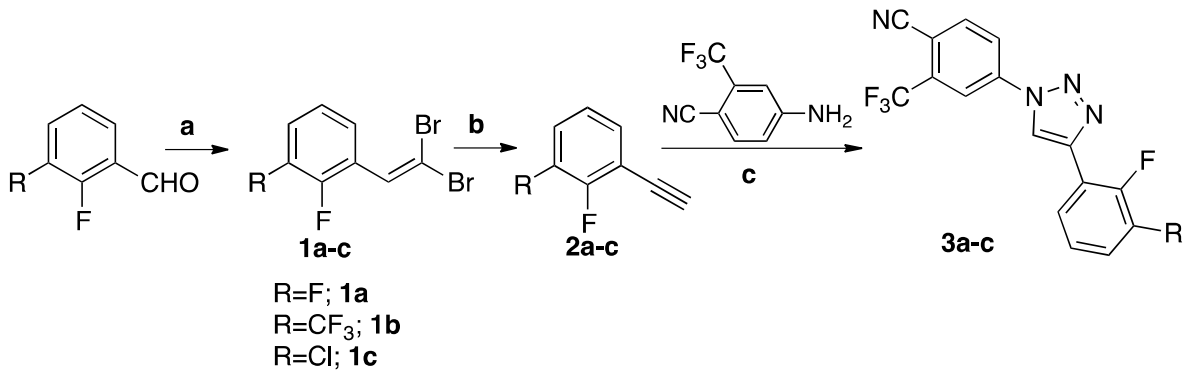

[a]Reagents: (a) Ph_3P, CBr_4, DCM, from 0°C to rt, 15', 72-99%; (b) n-BuLi, DIPA, THF, 0°C, 1h; -78°C, 3h; from -78°C to rt, 12h, 9-51%; (c) *t*-BuONO, $TMSN_3$, CH_3CN, from 0°C to rt, 2h; $CuSO_4$, Na-L-ascorbate, rt, 12h, 24-32%.

Compounds **5a**-**m**, corresponding to scaffold **II** (shown in Fig. 2) were prepared as depicted in Scheme 2. Phenols or thio-phenols were first alkylated by Williamson reaction with propargyl bromide to give terminal alkynes (**4a**-**j**) in quantitative yield.[37]

Alkyne **4k** was prepared in a two-step protocol, starting from 2-bromo-5-nitrobenzotrifluoride. The first step is the copper-catalyzed hydroxylation and the second step is the alkylation of the resulting phenol (**6)**. The terminal alkynes (**4a-k**) were then used as substrates for the subsequent cycloaddition with aromatic azides.

Scheme 2. Synthesis of one-spacer triazoles **5a-m**.[a]

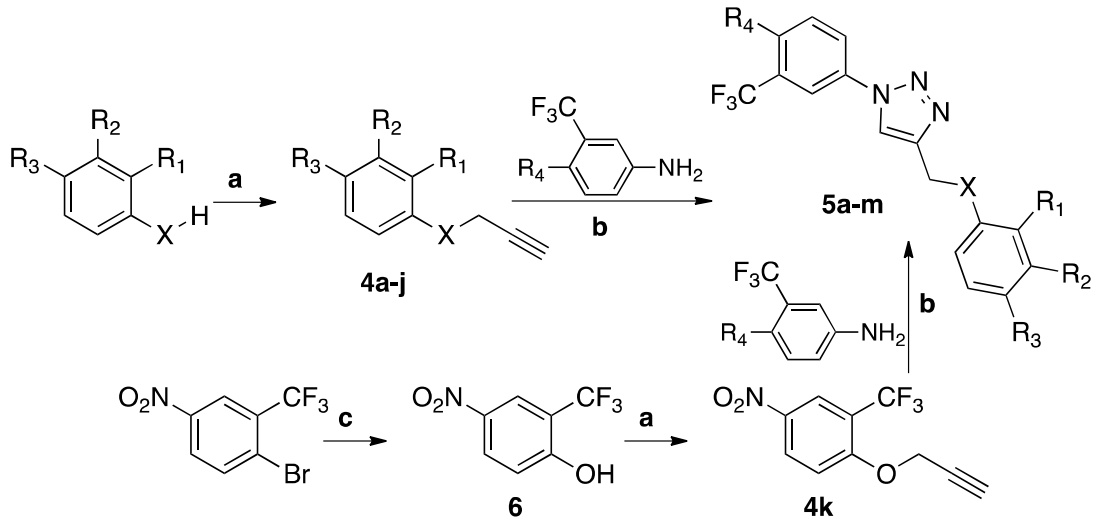

Compounds	R_1	R_2	R_3	R_4	X
5a	H	H	F	CN	S
5b	H	H	CN	CN	O
5c	H	H	F	CN	O
5d	H	CN	H	CN	O
5e	H	H	NO_2	CN	O
5f	H	H	CF_3	CN	O
5g	H	CF_3	H	CN	O
5h	H	CF_3	F	CN	O
5i	H	H	H	CN	O
5j	F	CF_3	H	CN	O
5k	CF_3	H	NO_2	CN	O
5l	CF_3	H	NO_2	H	O
5m	H	H	CN	Cl	O

[a]Reagents: (a) K_2CO_3, propargyl bromide, acetone, reflux, 24h, 79-100%; (b) *t*-BuONO, $TMSN_3$, CH_3CN, from 0°C to rt, 2h; $CuSO_4$, Na-L-ascorbate, rt, 12h, 16-87%; (c) CuI, phenanthroline, KOH, DMSO/H_2O, 100°C, 24h, 43%.

The synthesis of compounds **8a-d**, bearing linkers with variable length (n = 1, 3) is shown in Scheme 3. 4-Cyano-3-(trifluoromethyl)aniline was reacted with propargyl alcohol and 4-pentyn-1-ol to yield triazoles **7a** and **7b**, respectively These were then reacted with different phenols under Mitsunobu[38] conditions, to provide the corresponding ethers (**8a**-**8d**) in high yields.

Scheme 3. Synthesis of one-spacer triazoles **8a-d**.[a]

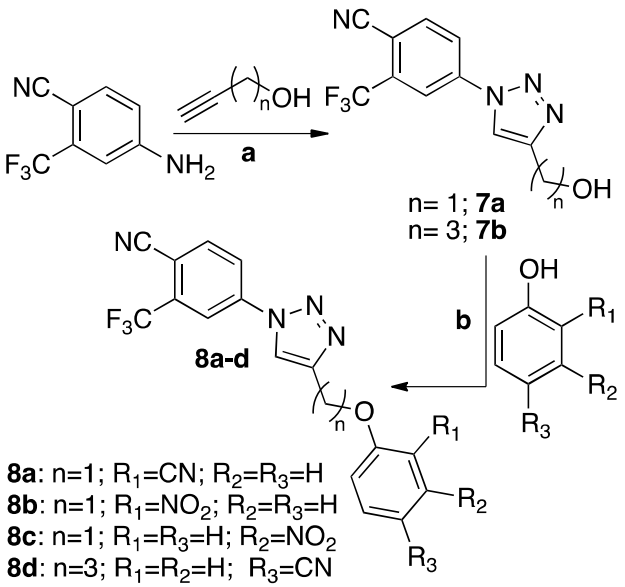

[a]Reagents: (a) *t*-BuONO, $TMSN_3$, CH_3CN, from 0°C to rt, 2h; $CuSO_4$, Na-L-ascorbate, rt, 12h, 69-89%; (b) Ph_3P, DIAD, THF, 0°C, 30'; rt, 12h, 24-77%.

In order to expand our SAR study, 1,4-disubstitued 1,2,3-triazoles were modified at position five of the triazole ring (Scheme 4). In particular, compound **5b** was reacted with n-BuLi and acetaldehyde to afford derivative **10** in good yield. In addition, an alternative CuAAC protocol was employed to prepare 5-iodo-1,4-disubstituted 1,2,3-triazole **11**, and CuI/NBS was used to generate *in situ* I^+, which readily undergoes the electrophilic substitution on the 5-position of the triazole ring.[39]

Scheme 4. Introduction of 5-substituent on 1,4-substitued 1,2,3-triazoles. [a]

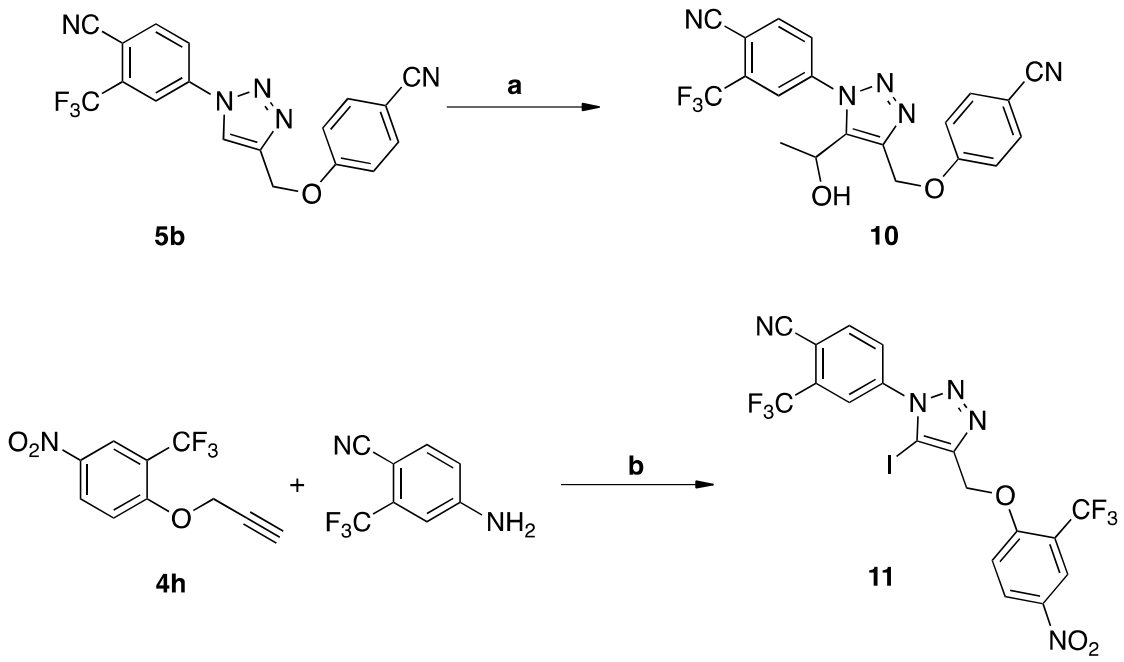

[a]Reagents: (a) n-BuLi, acetaldehyde, THF, -78°c to rt, 1h, 44%; (b) *t*-BuONO, $TMSN_3$, CH_3CN, from 0°C to rt, 2h; CuI, DIPEA, NBS, THF, rt, 12h, 35%.

The two-spacer triazole derivatives (**12a-c**) were synthesized as shown in scheme 5. Trifluoromethanesulfonyl azide (TfN_3) was prepared *in situ* from trifluoromethanesulfonic anhydride and sodium azide and was reacted with glycine methyl ester hydrochloride, the alkyne (**4a-c)**, $NaHCO_3$, sodium ascorbate and $CuSO_4$. Tris(benzyltriazolylmethyl)amine (TBTA) was also added to the mixture, to stabilize Cu(I). Upon microwave irradiation and maintaining the temperature at 80°C, the desired products **12a-c** were obtained in good yields (power 100 W, 5-10 min).[40]

The methyl esters **12a-c** were then hydrolyzed under basic conditions to the corresponding carboxylic acids **13a-c** and reacted with 4-cyano-3-(trifluoromethyl)aniline in a PCl_3-mediated microwave-assisted condensation, to afford the final compounds **14a-d**.[41]

Scheme 5. Synthesis of two-spacer triazoles **14a-d**.[a]

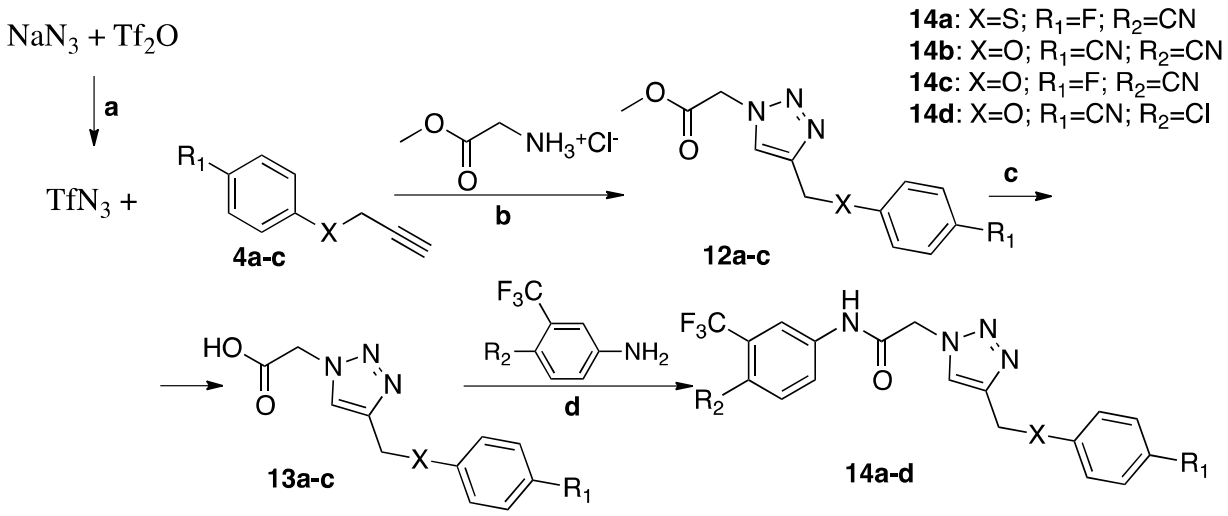

[a]Reagents: (a) DCM, 0°C, 2h, 100%; (b) $CuSO_4$, $NaHCO_3$, MeOH, rt, 30'; TBTA, Na-L-ascorbate, 80°C, 10', mw, 76-92%; (c)LiOH, THF/MeOH, rt, 12h, 88-100%; (d) PCl_3, CH_3CN, 100°C, 5', mw, 56-72%.

2.2. *In vitro* biological activity

PSA Expression. The antiandrogen activity of the newly synthesized triazole derivatives was initially screened *in vitro* using real-time quantitative reverse transcription-polymerase chain reaction (RT-qPCR). The activity of the compounds was defined by testing their ability to control and to lower PSA expression. To this purpose, we selected the AR-positive LNCaP cells,[42] a cell system widely used as a model of androgen-responsive growth. LNCaP cells were treated with 10 μM compounds for 24 h at 37°C and PSA mRNA levels were measured. Compared with untreated cells, the compounds generally reduce the PSA level (Fig. 3). In particular, we identified 10 compounds able to reduce PSA mRNA expression over 50%. No-spacer triazoles **3a-c**, (blue bars, Fig. 3) were found to be less active with a highest inhibition of 38% (**3a**). Compounds **14**, bearing two spacers (red bars, Fig. 3), showed modest activity, except for **14b** that produced 70% reduction in PSA mRNA expression level.

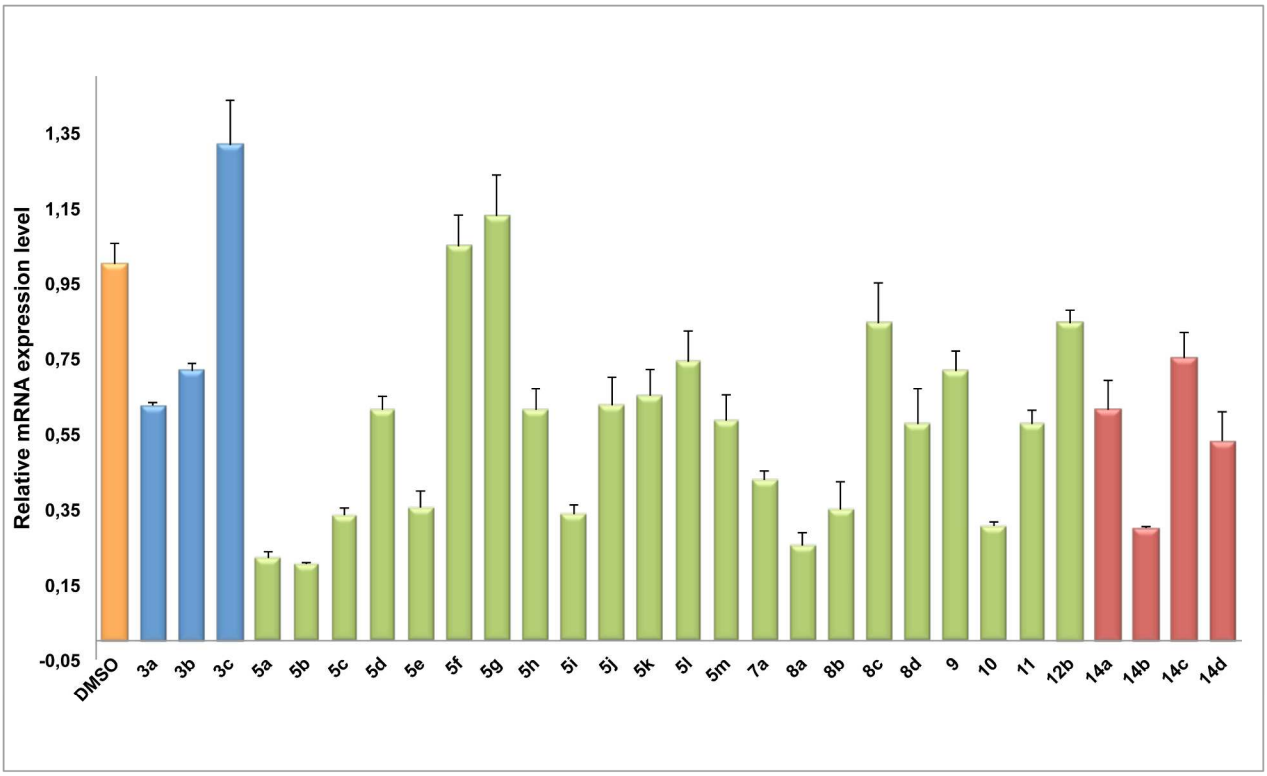

Figure 3. Evaluation of PSA mRNA levels after exposure of LNCaP cell lines to triazoles. Twenty-four hours after seeding, cells were treated for 24 h with 10 μM compounds. Cells were then collected, processed for mRNA extraction and analyzed using RT-qPCR. Blue bars: no-spacer triazoles (type I); Green bars: one-spacer triazoles (type II); Red bars two-spacer triazoles (type III).

One-spacer triazoles (green bars, Figure 3) showed good activity when the B ring was benzene (**5i**) or had *ortho*- or *para*-substituent (**5a-c**; **5e**; **8a-b** and **10**). In particular, the PSA down-regulation was over 65% for compounds **5a**, **5b**, **5c**, **5e**, **5i**, **8a**, **8b** and **10**. It is worth noting that a trifluoromethyl group on the B ring dramatically decreased compound activity (**5f**, **5g**, **5h**, **5j**, **5k**, **5l** and **11**). Moreover, a decreased efficacy was observed when the sulfur moiety of derivative **5a** was oxidized to sulphone (compound **9**, supporting information section). Furthermore, compound **12b**, lacking the A ring, was considerably less potent, suggesting that

this aromatic ring is crucial. Finally, further functionalization on the 5-position of the triazole e.g. **10** and **11**, did not significantly improve the ability to reduce PSA levels. Based on these findings, we summarized (Fig. 4), the effect of triazole ring substituents on PSA mRNA reduction.

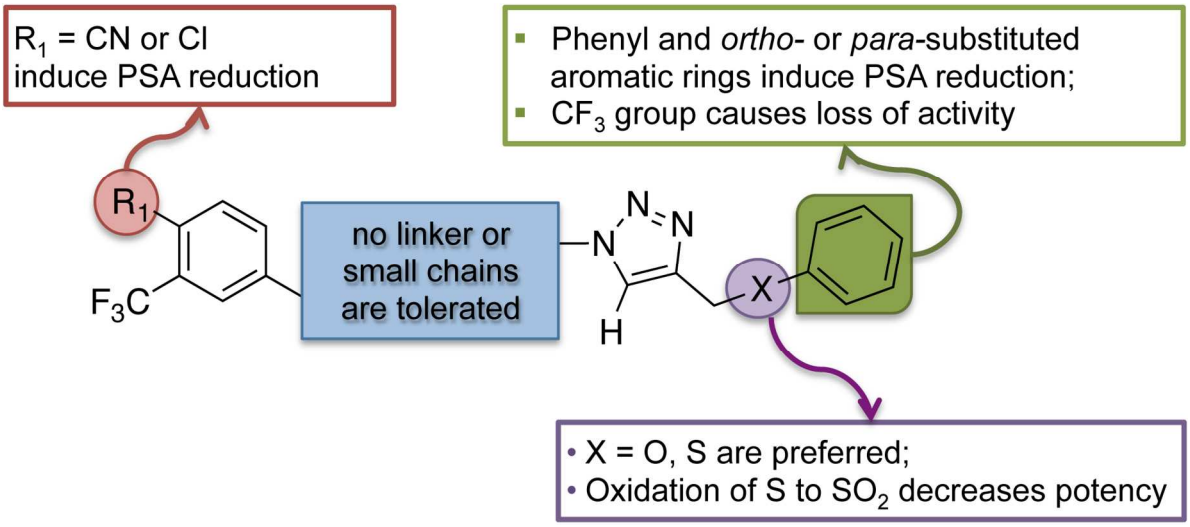

Figure 4. Influence of 1,4-triazole ring substituents on the PSA level reduction.

Cytotoxic Activity in vitro. On the basis of the PSA expression assay, some of the most active compounds (**5a**, **5c**, **5e**, **5i**, **7a**, **8a**, **8b** and **10** that inhibited PSA mRNA expression over 50%) were selected for cytotoxic experiments. Compounds **3a** (representative of no-spacer triazoles) and **14b** and **14d** (representatives of the two-spacer derivatives series) were also tested. Cytotoxic experiments were carried out using LNCaP and LNCaP-AR cell lines, the latter engineered to stably express high levels of AR, a condition considered representative of clinical AR gene amplification reported in 25−30% of patients with CRPC.[26,43] Cells were exposed to drug concentrations ranging from 0.02 μM to 20 μM for 144 hours using (*R*)-bicalutamide and enzalutamide as references. As reported in Figure 5 and Table 1, not all the compounds reached a cytotoxic activity toward the selected human PC cells.

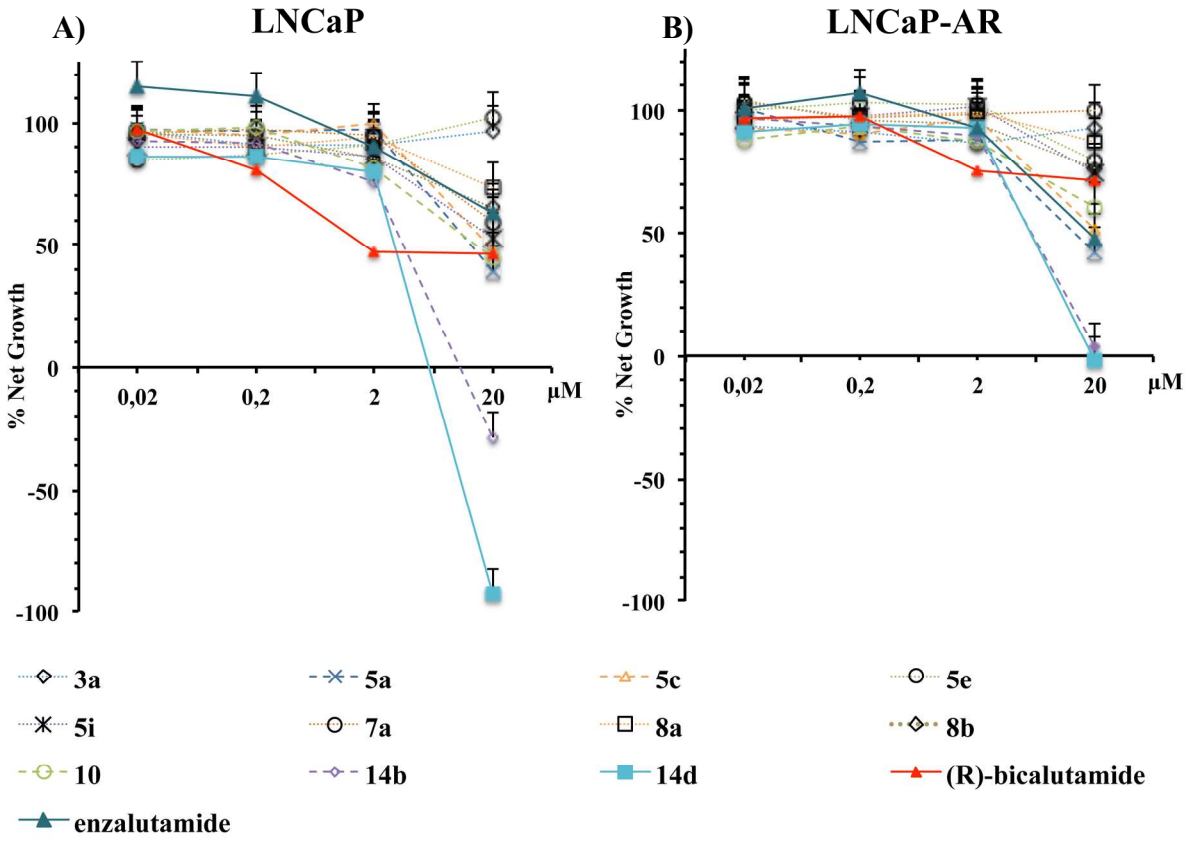

Figure 5. Cytotoxic activity of novel triazole derivatives against human PC LNCaP (A) and LNCaP-AR (B) cells. Twenty-four hours after seeding, cells were exposed to the compounds for 144 h to the compounds and cytotoxicity was measured using a sulforhodamine B (SRB) assay. (*R*)-bicalutamide and enzalutamide were used as references. The mean of three independent experiments is reported.

Table 1. Cytotoxic activity of (*R*)-bicalutamide, enzalutamide and triazole derivatives on LNCaP and LNCaP-AR cells.[a]

	GI_{50} value (μM)[b]		LC_{50} value (μM)[c]	
	LNCaP	LNCaP-AR	LNCaP	LNCaP-AR
(*R*)-bicalutamide	1.8±0.53	n.r.	n.r.	n.r.
enzalutamide	n.r.	18.88±1.89	n.r.	n.r.
5a	16.75±0.17	17.01±2.02	n.r.	n.r.
5c	19.23±0.37	n.r.	n.r.	n.r.
10	17.34±0.19	n.r	n.r.	n.r.
14b	6.42±0.23	10.30±1.47	n.r.	n.r.
14d	5.09±0.85	10.16±0.66	15.70±0.22	n.r

[a]Twenty-four hours after seeding, cells were exposed for 144 h to the compounds and cytotoxicity was measured using a sulforhodamine B (SRB) assay. [b]GI_{50} Growth Inhibition: is the concentration of compound producing 50% of maximal inhibition of cell proliferation; [c]LC_{50} Lethal Concentration: is the concentration of compound producing 50% cell death; n.r., not reached. Data represent mean values ± SD of three independent experiments.

In AR-mutated LNCaP cells, (*R*)-bicalutamide was the most effective compound (GI_{50} = 1.8 ± 0.53 μM), while only **5a**, **5c**, **10**, **14b** and **14d** inhibited cell proliferation with GI_{50} values ranging from about 5 μM to 19 μM. At the tested concentrations, only **14d** exhibited a cytocidal effect in LNCaP cells (LC_{50} = 15.70 ± 0.22 μM).

As expected, (*R*)-bicalutamide was ineffective in inhibiting LNCaP-AR cell proliferation. Conversely, **5a**, **14b** and **14d** showed higher cell growth inhibition as compared with enzalutamide (GI_{50} = 18.88 ± 1.89 μM) without reaching LC_{50} values. In particular, compounds **14b** (GI_{50} = 10.30 ± 1.47 μM) and **14d** (GI_{50} = 10.16 ± 0.66 μM) were the most potent derivatives of the series.

These findings suggested that the type III triazoles displayed the strongest cytotoxic effect, and compound **14d** was the most effective of the series.

Recently, the detection of androgen receptor splice variant 7 (AR-V7) mRNA in circulating tumor cells from men with advanced prostate cancer has been reported to associate with resistance to enzalutamide and abiraterone.[44] On the basis of these findings, CW22Rv1 cells, a prostate cancer cell model that constitutively expresses high levels of AR-V7,[45] were used to evaluate the antitumor activity *in vitro* of compound **14d**. (*R*)-bicalutamide and enzalutamide were used as references (Fig. 6).

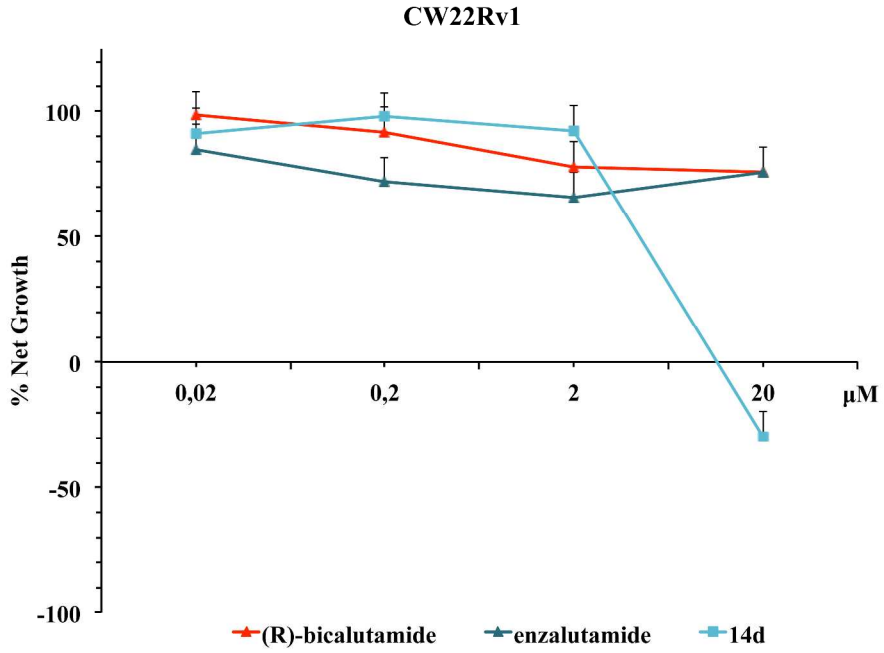

Figure 6. Cytotoxic activity of **14d** against human CW22Rv1 cells. Twenty-four hours after seeding, cells were exposed for 144 h to the compounds. The cytotoxic potency was measured using a sulforhodamine B (SRB) assay. (*R*)-bicalutamide and enzalutamide were used as references. The mean of three independent experiments is reported.

No significant difference in antitumor activity was observed for (*R*)-bicalutamide and enzalutamide on CW22Rv1 cells, while our newly synthesized **14d** compound resulted in 3.8-

and 4.4-fold more active than (*R*)-bicalutamide and enzalutamide, respectively (IC_{50} = 8.14 ± 0.90 μM). At the tested concentrations, only **14d** exhibited antiproliferative and cytocidal effects (GI_{50} = 8.25 ± 0.08 and LC_{50} = 15.70 ± 0.22 μM, Table 2).

None of the active compounds, filtered for Pan Assay Interference Compounds (PAINS)[46] using FAF-Drug3,[47] were already described.

Table 2. Cytotoxic activity of (*R*)-bicalutamide, enzalutamide and triazole derivative **14d** on CW22Rv1.[a]

	IC_{50} 72 h (μM)[b]	GI_{50} value 144 h (μM)[c]	LC_{50} value 144 h (μM)[d]
(*R*)-bicalutamide	31.29±1.83	n.r.	n.r.
enzalutamide	35.75±2.43	n.r.	n.r.
14d	8.14±0.90*	8.25±0.08	23.07±0.90

[a]Twenty-four hours after seeding, CW22Rv1 cells were exposed to the compounds for 72 h and 144 h. Seventy-two hours after exposure, cells were counted using a cell counter. [b]IC_{50} is defined as the concentration of compound causing 50% cell growth inhibition. To define [c]GI_{50} (Growth Inhibition: concentration of compound producing 50% of maximal inhibition of cell proliferation) and [d]LC_{50} (Lethal Concentration: concentration of compound producing 50% cell death) values, 144 h after compound exposure, cell proliferation was determined using a sulforhodamine B (SRB) assay. n.r., not reached. Data represent mean values ± SD of three independent experiments. *P<0.005 **14d** *vs* (*R*)-bicalutamide and enzalutamide.

2.3. *In vivo* Biological Activity

Based on these results, compound **14d** was selected for *in vivo*. CW22Rv1 cells ($5x10^6$ cells/mouse) were subcutaneously inoculated in the flank of CD-1 male nude (nu/nu) mice. The day after cell inoculation, mice were treated with 50 mg/Kg of **14d** according to the schedule qdx4-5/wx3w (every day for five days a week for three weeks). The second-generation androgen receptor antagonist enzalutamide was used as reference (50 mg/Kg, qdx5/wx3w). Compared with enzalutamide, **14d** was more active (Figure 7). As reported in Table 3, mice treated with

14d showed a 60% tumor volume inhibition. Finally, the treatment with **14d** was well tolerated, as no body weight loss was observed during or after the end of treatment.

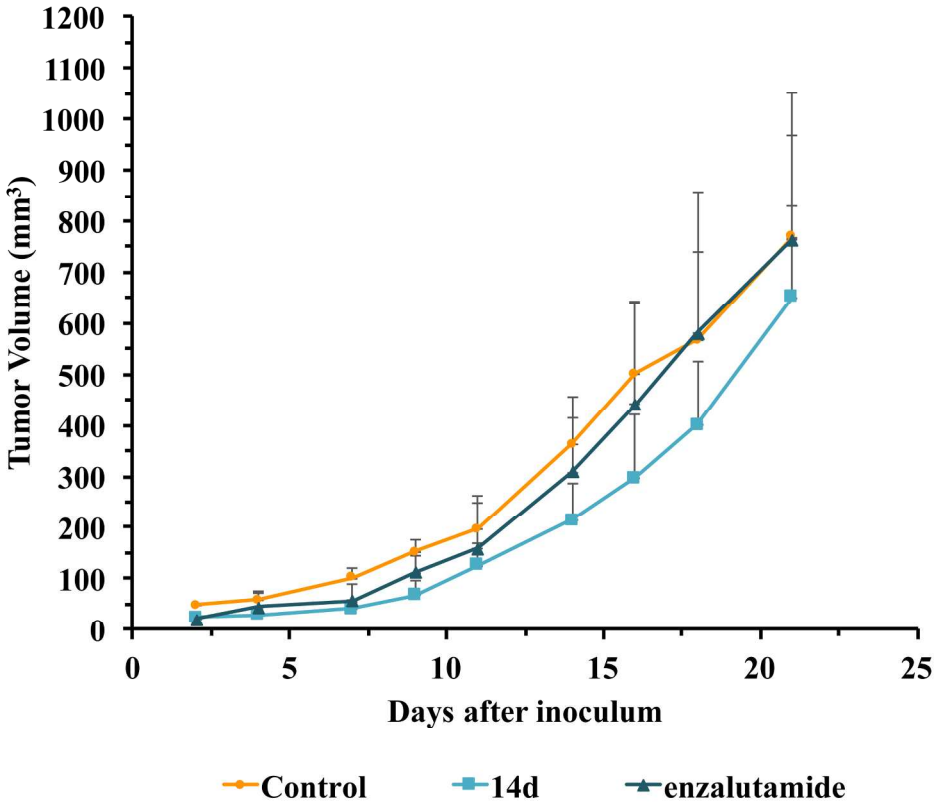

Figure 7. Antitumor activity of oral **14d** and enzalutamide against human prostate CW22Rv1 carcinoma tumor xenograft. CW22Rv1 cells ($5x10^6$/mouse) were injected into the right flank of the mice on day 0. Treatment started when tumors were not palpable (day 1). Drugs or vehicle (for Control group), were administrated orally at the dose of 50mg/kg according the qdx5/wx3w schedule. Tumor size was measured by caliper, and tumor volume calculated using: TV= a × b2/2, where a and b are the long and short diameters of the tumor, respectively. Points, mean from five mice per group; bars, SD.

Table 3. Antitumor activity of oral **14d** and enzalutamide on human prostate CW22Rv1 carcinoma cells xenografted s.c. in male nude mice.[a]

	TVI%max[b]	BWL%[c]	Tox[d]
enzalutamide	43(7)	0	0/5
14d	60*(7)	0	0/5

[a]Cells ($5x10^6$/mouse) were injected into the right flank of the mice on day 0. Treatment started when tumors were not palpable (day 1). Drugs were administrated at the dose of 50mg/kg according the qdx5/wx3w schedule. [b]The highest value of TVI%. In parentheses, the day on which it was assessed. [c]Body weight loss % induced by drug treatment. [d]Dead/treated mice. *P<0.05 by Student's t test *vs* solvent-treated mice.

2.4. Molecular Modeling

In order to better elucidate the mechanism of compound **14d** antagonism at the molecular level, we performed molecular modeling calculations and compared them to those of (*R*)-bicalutamide and enzalutamide. At first, a rigid docking simulation was performed, however this procedure failed to provide a binding pose for both enzalutamide and compound **14d**. The analysis of the scaffolds overlaying between enzalutamide and **14d** with (*R*)-bicalutamide, revealed that their lower molecular flexibility could prevent their suitable fitting in the active site cavity. This finding clearly indicated the possible occurrence of conformational changes in the active site geometry induced by the bound ligand, the so-called "induced fit" mechanism. Therefore, to further elucidate the binding site flexibility, binding modes of active compounds were generated through Glide/Induced Fit Docking protocol (IFD), which exhaustively considers all possible binding modes and the associated conformational changes within the receptor active site. Figure 7 reports the predicted binding modes of the three molecules.

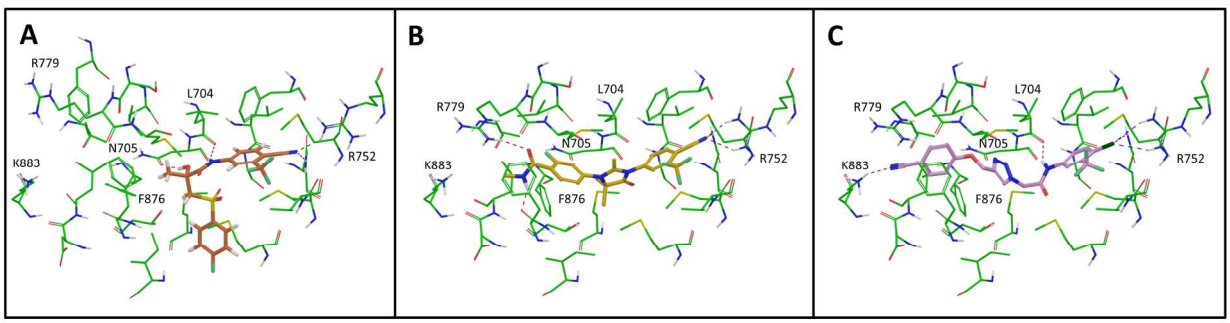

Figure 8. Putative binding mode of AR modulators. Predicted binding mode of (*R*)-bicalutamide (A), enzalutamide (B) and compound **14d** (C). Hydrogen bonds are represented as red dotted lines. Binding pose of *(R)*-bicalutamide was obtained through rigid docking starting from AR crystallographic structures (pdb code 2AXA), whereas poses of enzalutamide and **14d** were obtained from IFD simulations.

The pose of (*R*)-bicalutamide (Fig. 8-A) is consistent with crystallographic complexes previously reported.[48] In particular, the cyano group on the A ring forms an hydrogen bond with the side chain of Arg752, as well as with the amide nitrogen and the chiral hydroxyl group with Leu704 and Asn705 respectively, while the B ring of the ligand is enclosed in an hydrophobic pocket formed by Trp741, Met742, Met745 and Met895. The IFD calculation suggests that small adjustments in the position of the side chain of Arg779, Phe876, Phe891 and Leu880 could allow an effective binding of enzalutamide and **14d** (Fig. 8-B and C). In both compounds the A ring establishes a hydrogen bond network similar to (*R*)-bicalutamide, even if the hydrogen bond formed by the cyano group is replaced by a halogen bond in **14d**, while the B ring is located in a different pocket, formed as a result of the conformational rearrangement of the active site. Enzalutamide forms additional hydrogen bond interactions through its amide group on ring B with the side chain of Arg779 and the backbone carbonyl of Phe876. Similarly, **14d** keeps the interaction between the amide nitrogen and the side chain of Leu704, and forms an additional hydrogen bond between the side chain of Lys883 and the cyano group on ring B, and a Pi-Pi stacking interaction with Phe876.

3. Conclusions

Herein we report the synthesis and biological *in vitro* evaluation of a novel class of bicalutamide-like molecules as androgen receptor antagonists. Based on the consideration that

commercially available non-steroidal antiandrogens show a common scaffold consisting of two aromatic rings linked by a linear or a cyclic spacer, we developed a facile and efficient CuAAC process that allows to access to a wide library of new triazole derivatives with antagonist activity against the androgen receptor. Collectively, the biological data demonstrate that the introduction of the triazole ring as an amide bond isoster is a promising option toward the improvement of the AR-antagonist behavior. Overall, compound **14d** proved to be the most promising of the series, being active toward three different cell prostate cancer lines, including LNCaP, LNCaP-AR and CW22Rv1. Although less effective than (*R*)-bicalutamide on the LNCaP cell line, **14d** exhibited a superior antitumor activity towards LNCaP-AR, a cell line over-expressing the AR and representative of 25-30% of patients with CRPC. Furthermore, **14d** was more active than (*R*)-bicalutamide and enzalutamide on CW22Rv1 cells, a model cell system representatives of enzalutamide resistance associated with the expression of AR-V7 in men suffering from advanced prostate cancer. Importantly, the results observed *in vitro* are corroborated by the superior antitumor potency showed *in vivo* by **14d** in comparison to enzalutamide (60 *vs* 43% TVI%) on xenografted CW22Rv1 tumors. Collectively, the results of induced fit docking suggest that the aromatic rings are able to establish interaction networks similar to (*R*)-bicalutamide, confirming that the triazole ring keeps a suitable conformation. In conclusion, the significant *in vitro* and *in vivo* antitumor activity shown by **14d** highlights its potential usefulness in the treatment of advanced human prostate cancer.

4. Experimental section

4.1 General Chemistry Methods. All reagents were used as obtained from commercial sources unless otherwise indicated. Solvents were dried over standard drying agents and freshly distilled prior to use. Deionized water was obtained with the Milli-Q Millipore Water Purification System

and is referred to as milliQ water throughout the paper. All microwave reactions were performed in a CEM Discover reactor. The ^{1}H and ^{13}C NMR spectra were recorded on Varian spectrometers (400 and 500 MHz for ^{1}H, 100 and 125 MHz for ^{13}C). Deuterated chloroform was used as the solvent for NMR experiments, unless otherwise stated. ^{1}H chemical shifts values (δ) are referenced to the residual non-deuterated components of the NMR solvents (δ = 7.26 ppm for $CHCl_3$ and δ = 3.31 ppm for CHD_2OD, etc.). The ^{13}C chemical shifts (δ) are referenced to $CDCl_3$ (central peak, δ = 77.0 ppm), CD_3OD (δ = 49.3 ppm), etc. as the internal standard. Optical rotation was detected on an ADP220 Automatic polarimeter from Bellingham & Stanley Limited. Mass spectra were measured in positive mode electrospray ionization (ESI). ESI-HRMS was acquired on an Agilent Dual ESI Q TOF 6520, in positive-ion mode, using methanol. Flash chromatography was performed on Teledyne Isco CombiFlash® Rf 200 using RediSep® Normal-phase Silica Flash Columns (230-400 mesh). TLC was performed on silica gel 60 F254 plastic sheets. Purity of prepared compounds was determined by HPLC-UV analysis (Waters 600 HPLC connected with Photodiode Array Detector 996). Pure (*R*)-bicalutamide (the active enantiomer of the non-steroidal antiandrogen, Casodex®) was straightforwardly synthesized by highly diastereoselective procedure,[49] and enzalutamide was purchased from Vinci-Biochem Srl (Florence, Italy). All compounds tested in biological assay were >95%. Purity of intermediates was >90%, unless otherwise stated. UV/Vis spectra were registered on a Agilent Cary 100 spectrophotometer.

4.2. Synthetic procedures. 4.2.1. General procedure for Williamson reaction. Method B: Synthesis of terminal alkynes ***4b-k***. A round bottom flask equipped with a magnetic stir bar was charged with phenol (1.0 equiv), K_2CO_3 (4.0 equiv), propargyl bromide (80% wt toluene, 4.0 equiv) and acetone (2 mL/mmol phenol). The mixture was heated to reflux for 24 hours and

cooled to rt. The solvent was removed under pressure and water was added. The heterogeneous mixture was extracted twice with EtOAc and the combined organic layers were dried over Na_2SO_4, filtered and concentrated. Characterization exemplified by *4-(prop-2-yn-1-yloxy)benzonitrile (**4b**).* The title compound was prepared using 4-cyanophenol. The yellow solid didn't need any further purification, quantitative yield. ^{1}H NMR (400 MHz, $CDCl_3$) δ 7.63–7.60 (m, 2H), 7.06–7.03 (m, 2H), 4.76 (d, *J* = 2.4 Hz, 2H), 2.57 (t, *J* = 2.4, Hz, 1H). ^{13}C NMR (100 MHz, $CDCl_3$) δ 160.6, 133.9, 119.0, 115.6, 104.9, 76.6, 65.8, 55.9. HRMS (*m/z*): calcd for $C_{10}H_7NO$ $[M]^+$, 157.0528; found: 157.0528.

*4.2.2. General procedure for microwave-assisted click chemistry: synthesis of triazoles (**12a-c**).* NaN_3 (6.0 equiv) was dissolved in H_2O (1 mL x 0.4 g NaN_3). At 0°C Tf_2O (3.0 equiv) in CH_2Cl_2 (1 mL x 0.4 g NaN_3) was added dropwise to the vigorously stirred solution. After 2 hours at 0°C, the aqueous phase was once extracted with the same volume of CH_2Cl_2. The combined organic phase was washed with saturated $NaHCO_3$ solution and used without further purification.

In a microwave reaction vial, glycine methyl ester hydrochloride (1.0 equiv), $CuSO_4 \cdot 5H_2O$ (2 mol%) and $NaHCO_3$ (2.0 equiv) were dissolved in the same volume of water as the volume of the TfN_3 solution to be employed. The TfN_3 solution was added to the mixture, followed by methanol until the solution became homogeneous. The reaction was stirred at rt for 30 min, then alkyne (1.0 equiv), TBTA (5 mol%) and sodium L-ascorbate (10 mol%) were added and the tube was sealed and heated at 80°C for 10 min by MW irradiation. The reaction mixture was diluted with water and then extracted with EtOAc. The crude was purified by flash chromatography. Characterization exemplified by *Methyl 2-(4-((4-cyanophenoxy)methyl)-1H-1,2,3-triazol-1-yl)acetate (**12b**).* The title compound was prepared using alkyne **4b** and following the general

method. The crude material was purified on a silica gel column eluted with 0-40% ethyl acetate in hexane, affording a white solid, yield = 92%. ^{1}H NMR (400 MHz, $CDCl_3$) δ 7.79 (s, 1H), 7.57–7.53 (m, 2H), 7.05–7.01 (m, 2H), 5.24 (s, 2H), 5.18 (s, 2H), 3.78 (s, 3H). ^{13}C NMR (100 MHz, $CDCl_3$) δ 166.5, 161.3, 143.3, 133.9, 124.4, 119.0, 115.4, 104.4, 61.8, 53.04, 50.6. HRMS (*m/z*): calcd for $C_{13}H_{12}N_4O_3$ $[M]^+$, 272.0909; found 272.0911.

*4.2.3. General procedure for hydrolysis of methyl ester (**13a-c**).* To a solution of ester (1.0 equiv) in THF (3.3 mL/mmol ester) and MeOH (2 mL/mmol ester) was added an aqueous 1.0M LiOH solution (2.0 equiv). The resulting mixture was stirred at room temperature overnight. The reaction mixture was neutralized with HCl 1N. The aqueous phase was extracted with EtOAc and the combined organic layers were washed with brine, dried and evaporated. The white solid didn't need any further purification. Characterization exemplified by *2-(4-((4-cyanophenoxy)methyl)-1H-1,2,3-triazol-1-yl)acetic acid (**13b**).* The title compound was prepared using ester **12b** and following the general method, quantitative yield. ^{1}H NMR (400 MHz, CD_3OD) δ 8.14 (s, 1H), 7.68–7.64 (m, 2H), 7.19–7.15 (m, 2H), 5.30 (s, 2H), 5.27 (s, 2H). ^{13}C NMR (100 MHz, CD_3OD) δ 169.8, 163.3, 144.3, 135.4, 127.3, 120.1, 117.0, 105.4, 62.7, 51.8. HRMS (*m/z*): calcd for $C_{12}H_{10}N_4O_3$ $[M]^+$, 258.0753; found 258.0755.

*4.2.4. General procedure for synthesis of triazoles **14a-d**.* To a solution of aniline (1.01 equiv) and carboxylic acid (1.0 equiv) in dry CH_3CN (10 mL/mmol aniline), PCl_3 (1.0 equiv) was added. The tube was sealed and heated at 100°C for 5 min by microwave irradiation (standard method), then the mixture was quenched with few drops of water. The reaction mixture was poured on a pre-packed basic alumina column and eluted with CH_2Cl_2/MeOH: 98/2. Characterization exemplified by *N-(4-chloro-3-(trifluoromethyl)phenyl)-2-(4-((4-cyanophenoxy)methyl)-1H-1,2,3-triazol-1-yl)acetamide (**14d**).* The title compound was obtained

as a white solid, starting from acid **13b** and 4-chloro-3-(trifluoromethyl)aniline and following the general method (yield = 72%). ^{1}H NMR (400 MHz, CD_3OD) δ 8.20 (s, 1H), 8.08 (d, *J* = 2.8 Hz, 1H), 7.79 (dd, *J* = 8.4, 2.4 Hz, 1H), 7.69–7.65 (m, 2H), 7.55 (d, *J* = 8.8 Hz, 1H), 7.20–7.17 (m, 2H), 5.39 (s, 2H), 5.30 (s, 2H). ^{13}C NMR (100 MHz, CD_3OD) δ 166.3, 163.4, 144.3, 138.9, 135.4, 133.4, 129.7 (q, *J* = 31.7 Hz), 127.8, 127.5, 125.4, 124.2 (q, *J* = 271.1 Hz), 120.2, 119.9 (q, *J* = 5.6 Hz), 117.0, 105.5, 62.8, 53.6. HRMS (*m/z*): calcd $C_{19}H_{13}ClF_3N_5O_2$ $[M]^+$, 435.0710; found 435.0705.

4.3. Bioassays. 4.3.1. Cell Lines. The human prostate cancer cell line LNCaP was obtained from the American Type Culture Collection (Manassas, VA, USA). The LNCaP-AR cell line, derived from LNCaP and engineered to stably express high levels of AR, was kindly provided by Dr. Charles L. Sawyers (Howard Hughes Medical Institute Investigator at Memorial Sloan Kettering Cancer Center in New York, NY; U.S.A. The cells were maintained in RPMI medium supplemented with 10% fetal bovine serum (FBS) and 1% glutamine. CW22Rv1 cells were cultured in RPMI 1640 containing 10% FBS and 1% glutamine. Cell lines were periodically checked for mycoplasma contamination by MycoAlert mycoplasma detection kit (Lonza).

4.3.2. Quantitative Real-Time Reverse-Transcription Polymerase Chain Reaction. LNCaP cells were incubated with the corresponding compounds for 24 h at 37 ºC. RNA was isolated from cells using the RNeasy mini kit (Qiagen). cDNA was generated using equal concentrations of RNA and the Taqman High Capacity Reverse Transcription kit in the GeneAmp PCR System 9700 machine (Applied Biosystems). Diluted cDNA was combined with the forward primer, reverse primer, SYBR Green PCR Master Mix and RNAse-free water in a 96-well plate. Analysis of mRNA expression was carried out using the ABI 7500 Real-Time PCR System (Applied Biosystems). All samples were normalized to the level of 18S ribosomal RNA (rRNA).

The threshold cycles (Ct) for the control (rRNA) and gene of interest were determined and relative RNA levels were calculated by the comparative Ct method. Real-time RT-qPCR experiments were performed in triplicate with the following primers:

PSA

forward 5'-GCAGCATTGAACCAGAGGAGTT-3'

reverse 5'-CACGTCATTGGAAATAACATGGA-3'

18S rRNA

forward 5'-AGTCCCTGCCCTTTGTACACA-3'

reverse 5'-CGATCCGAGGGCCTCACTA-3'

4.3.3. In Vitro Chemosensitivity Assay. Sulforhodamine B (SRB) assay was used according to the method by Skehan et al.[50] Briefly, cells were collected by trypsinization, counted, and plated at a density of 5000 cells/well (LNCAP and LNCAP-AR cell lines) or 1700 cells/well (CW22Rv1 cell line) in 96-well flat-bottomed microtiter plates (100 μL of cell suspension/well). Twenty-four hours after seeding, the cells were exposed to the drugs for 144 h (concentration range 0.02-20 μM). Experiments were run in octuplicate, and each experiment was repeated three times. The optical density of cells was determined at a wavelength of 490 nm by a colorimetric plate reader.

Growth inhibition and cytocidal effect of drugs were calculated according to the formula reported by Monks et al.:[51] $[(OD_{treated} - OD_{zero})/(OD_{control} - OD_{zero})]$ X 100%, when $OD_{treated}$ is > OD_{zero}. If $OD_{treated}$ is below OD_{zero}, then cell killing has occurred. OD_{zero} depicts the cell number at the moment of drug addition, $OD_{control}$ reflects the cell number in untreated wells, and $OD_{treated}$

reflects the cell number in treated wells on the day of the assay. GI_{50} and LC_{50} were defined as the concentration inhibiting cell growth by 50% and causing the 50% of cell killing, respectively.

Cytotoxic potency on CW22Rv1 was also assessed by growth inhibition assay. Twenty-four hours after seeding, cells were exposed to the drugs (concentration range 0.5−100 μM) and counted 72 h later by coulter counter. IC_{50} is defined as the drug concentration causing 50% cell growth inhibition, determined by dose−response curves. Experiments were performed in triplicate.

4.3.4. In Vivo Experiments. Eight week-old CD-1 male nude (nu/nu) mice (Charles River Laboratories, Calco, Italy) were used. Experiments were carried out at the Animal Facility of Fondazione IRCCS Istituto Nazionale dei Tumori of Milan, Italy. The procedures were in compliance with our institutional animal care guidelines and with international directives in accordance with Italian law and approval by the Ministry of Health. The animals were euthanized by cervical dislocation when tumors reached a mean volume of $800mm^3$. For antitumor activity experiments, CW22Rv1 prostate cancer cells ($5x10^6$ cells/mouse in 100 μL of saline) were subcutaneously injected in the right flank of the mice. Animals were randomized, divided in groups (5 mice per group) and, starting the day after cell injection, treated orally by gavage with 50 mg/Kg of enzalutamide or **14d** at a volume of 10mL/kg of body weight, every day for five days a week for three weeks (qdx5/wx3w). All the compounds were dissolved in DMSO and Cremophor and suspended in PBS (10+5+85%). Control mice were treated with vehicle for the same treatment period. Tumor size was measured by caliper, and tumor volume calculated using the following formula: a × b2/2, where a and b are the long and short diameters of the tumor, respectively.

4.4. Theoretical Calculations Method. 4.4.1. Protein Preparation. The X-ray coordinates of human androgen receptor ligand binding domain in complex with S-1 were extracted from the Protein Data Bank (PDB code 2AXA)[16129672]. The structure was then processed with the Protein Preparation Wizard tool as included in the Schrödinger software suite (Schrödinger Release 2014-4, Schrödinger, LLC, New York, NY, 2014); this tool automatically sets charges and correct atom types, bond orders and the orientation of any misoriented groups (such as amide groups of Asn and Gln). The ligand and water molecules were removed, and an exhaustive sampling of the orientations of groups, whose hydrogen bonding network needs to be optimized, was performed. Finally, the protein structure was refined to relieve steric clashes with a restrained minimization with the OPLS2005 force field until a final rmsd of 0.020 Å with respect to the input protein coordinates.

4.4.2. Docking. Docking studies were performed using the software Glide (Schrödinger Release 2014-4, Schrödinger, LLC, New York, NY, 2014). The protein structure, prepared as described above, was used to build the energy grid. A docking grid was obtained by centering a 25 Å box in the centroid of the bound ligand, as present in the template crystallographic structure of the human AR. All waters were removed from the grid. Standard precision (SP) docking was used to perform a first round of virtual screening, and poses were further refined with the extra-precision (XP) docking.

4.4.3. Induced Fit protocol. An initial Glide SP docking of each ligand was performed by using a softened potential, i.e., a van der Waals radius scaling factor of 0.50 for receptor/ligand atoms with a partial atomic charge (absolute value) less than 0.15, the metal constraint, and a number of 1000 poses per ligand to be energy minimized on the OPLS-AA nonbonded-interaction grid, as reported above. One hundred poses were saved for each ligand and submitted to the subsequent

Prime side-chain orientation prediction of residues within a shell of 6 Å around each ligand. After the Prime minimization of the selected residues and the ligand for each pose, a Glide redocking of each protein–ligand complex structure within 30 kcal/mol of the lowest energy structure was performed. Finally, binding energy (IFDScore) for each output pose was estimated and the poses for each protein–ligand complex were visually inspected.

ASSOCIATED CONTENT

Supporting Information. The Supporting Information is available free of charge on the ACS Publications website at DOI: detailed synthetic procedures, characterization data, ^{1}H and ^{13}C NMR spectra of all final compounds (pdf). Molecular formula strings (csv).

AUTHOR INFORMATION

Corresponding Author

*Dr. Claudia Ferroni – Italian National Research Council - Institute of Organic Synthesis and Photoreactivity Via P. Gobetti, 101 40129 Bologna (ITALY). Phone +390516398286; Fax +390516398349 Email claudia.ferroni@isof.cnr.it

*Dr. Greta Varchi – Italian National Research Council - Institute of Organic Synthesis and Photoreactivity Via P. Gobetti, 101 40129 Bologna (ITALY). Phone +390516398283; Fax +390516398349 Email greta.varchi@isof.cnr.it

Author Contribution

Claudia Ferroni and Antonella Pepe equally contributed to this work.

ABBREVIATIONS

PC, prostate cancer; AR, androgen receptor; LBD, ligand-binding domain; ADT, androgen-deprivation therapy; AIPC, androgen-independent prostate cancer; CRPC, castration-resistant prostate cancer; T, testosterone; DHT, dihydrotestosterone; PSA, prostate-specific antigen; CuAAC, copper-alkyne-azide-cycloaddition; LDA lithium diisopropylamide; *t*-BuONO, *tert*-butyl nitrite; $TMSN_3$, azidotrimethylsilane; n-BuLi, butyllithium; NBS, N-Bromosuccinimide; TfN_3, Trifluoro-methanesulfonyl azide; TBTA, Tris(benzyltriazolylmethyl)amine, SRB, sulforhodamine B; AR-V7, androgen receptor splice variant 7, PAINS, Pan Assay Interference Compounds; IFD, Induced Fit Docking protocol.

References

(1) Torre, L. A.; Bray, F.; Siegel, R. L.; Ferlay, J.; Lortet-tieulent, J.; Jemal, A. Global Cancer Statistics, 2012. *Ca-Cancer J. Clin.* **2015**, *65* (2), 87–108.

(2) Chen, C. D.; Welsbie, D. S.; Tran, C.; Baek, S. H.; Chen, R.; Vessella, R.; Rosenfeld, M. G.; Sawyers, C. L. Molecular Determinants of Resistance to Antiandrogen Therapy. *Nat. Med.* **2003**, *10* (1), 33–39.

(3) Tian, X.; He, Y.; Zhou, J. Progress in Antiandrogen Design Targeting Hormone Binding Pocket to Circumvent Mutation Based Resistance. *Front. Pharmacol.* **2015**, *6* (MAR), 1–11.

(4) Scher, H. I. Biology of Progressive, Castration-Resistant Prostate Cancer: Directed Therapies Targeting the Androgen-Receptor Signaling Axis. *J. Clin. Oncol.* **2005**, *23* (32), 8253–8261.

(5) Wang, Q.; Li, W.; Zhang, Y.; Yuan, X.; Xu, K.; Yu, J.; Chen, Z.; Beroukhim, R.; Wang, H.; Lupien, M.; Wu, T.; Regan, M. M.; Meyer, C. A.; Carroll, J. S.; Manrai, A. K.; Jänne, O. A.;

Balk, S. P.; Mehra, R.; Han, B.; Chinnaiyan, A. M.; Rubin, M. A.; True, L.; Fiorentino, M.; Fiore, C.; Loda, M.; Kantoff, P. W.; Liu, X. S.; Brown, M. Androgen Receptor Regulates a Distinct Transcription Program in Androgen-Independent Prostate Cancer. *Cell* **2009**, *138* (2), 245–256.

(6) Visakorpi, T.; Hyytinen, E.; Koivisto, P.; Tanner, M.; Keinänen, R.; Palmberg, C.; Palotie, A.; Tammela, T.; Isola, J.; Kallioniemi, O. P. In Vivo Amplification of the Androgen Receptor Gene and Progression of Human Prostate Cancer. *Nat. Genet.* **1995**, *9* (4), 401–406.

(7) Veldscholte, J.; Ris-Stalpers, C.; Kuiper, G. G.; Jenster, G.; Berrevoets, C.; Claassen, E.; van Rooij, H. C.; Trapman, J.; Brinkmann, A. O.; Mulder, E. A Mutation in the Ligand Binding Domain of the Androgen Receptor of Human LNCaP Cells Affects Steroid Binding Characteristics and Response to Anti-Androgens. *Biochem. Biophys. Res. Commun.* **1990**, *173* (2), 534–540.

(8) Linja, M. J.; Savinainen, K. J.; Saramäki, O. R.; Tammela, T. L.; Vessella, R. L.; Visakorpi, T. Amplification and Overexpression of Androgen Receptor Gene in Hormone-Refractory Prostate Cancer. *Cancer Res.* **2001**, *61* (9), 3550–3555.

(9) Grasso, C. S.; Wu, Y.-M.; Robinson, D. R.; Cao, X.; Dhanasekaran, S. M.; Khan, A. P.; Quist, M. J.; Jing, X.; Lonigro, R. J.; Brenner, J. C.; Asangani, I. A.; Ateeq, B.; Chun, S. Y.; Siddiqui, J.; Sam, L.; Anstett, M.; Mehra, R.; Prensner, J. R.; Palanisamy, N.; Ryslik, G. A.; Vandin, F.; Raphael, B. J.; Kunju, L. P.; Rhodes, D. R.; Pienta, K. J.; Chinnaiyan, A. M.; Tomlins, S. A. The Mutational Landscape of Lethal Castration-Resistant Prostate Cancer. *Nature* **2012**, *487* (7406), 239–243.

(10) De Maeseneer, D. J.; Van Praet, C.; Lumen, N.; Rottey, S. Battling Resistance Mechanisms in Antihormonal Prostate Cancer Treatment: Novel Agents and Combinations. *Urol. Oncol. Semin. Orig. Investig.* **2014**, *33* (7), 310–321.

(11) Ammannagari, N.; George, S. Anti-Androgen Therapies for Prostate Cancer : A Focused Review. *Am J Hematol Oncol.* **2014**, *11* (2), 15–19.

(12) Delaere, K. P.; Van Thillo, E. L. Flutamide Monotherapy as Primary Treatment in Advanced Prostatic Carcinoma. *Semin. Oncol.* **1991**, *18* (5 Suppl 6), 13–18.

(13) Kolvenbag, G. J.; Blackledge, G. R.; Gotting-Smith, K. Bicalutamide (Casodex) in the Treatment of Prostate Cancer: History of Clinical Development. *Prostate* **1998**, *34* (1), 61–72.

(14) Bohl, C. E.; Gao, W.; Miller, D. D.; Bell, C. E.; Dalton, J. T. Structural Basis for Antagonism and Resistance of Bicalutamide in Prostate Cancer. *Proc. Natl. Acad. Sci. U. S. A.* **2005**, *102* (17), 6201.

(15) Scher, H. I.; Beer, T. M.; Higano, C. S.; Anand, A.; Taplin, M. E.; Efstathiou, E.; Rathkopf, D.; Shelkey, J.; Yu, E. Y.; Alumkal, J. Antitumour Activity of MDV3100 in Castration-Resistant Prostate Cancer: A Phase 1-2 Study. *Lancet* **2010**, *375* (9724), 1437–1446.

(16) Tran, C.; Ouk, S.; Clegg, N. J.; Chen, Y.; Watson, P. A.; Arora, V.; Wongvipat, J.; Smith-Jones, P. M.; Yoo, D.; Kwon, A.; Wasielewska, T.; Welsbie, D.; Chen, C. D.; Higano, C. S.; Beer, T. M.; Hung, D. T.; Scher, H. I.; Jung, M. E.; Sawyers, C. L. Development of a Second-Generation Antiandrogen for Treatment of Advanced Prostate Cancer. *Science (80-.).* **2009**, *324* (5928), 787–790.

(17) Clegg, N. J.; Wongvipat, J.; Joseph, J. D.; Tran, C.; Ouk, S.; Dilhas, A.; Chen, Y.; Grillot, K.; Bischoff, E. D.; Cai, L.; Aparicio, A.; Dorow, S.; Arora, V.; Shao, G.; Qian, J.; Zhao, H.; Yang, G.; Cao, C.; Sensintaffar, J.; Wasielewska, T.; Herbert, M. R.; Bonnefous, C.; Darimont, B.; Scher, H. I.; Smith-Jones, P.; Klang, M.; Smith, N. D.; De Stanchina, E.; Wu, N.; Ouerfelli, O.; Rix, P. J.; Heyman, R. A.; Jung, M. E.; Sawyers, C. L.; Hager, J. H. ARN-509: A Novel Antiandrogen for Prostate Cancer Treatment. *Cancer Res.* **2012**, *72* (6), 1494–1503.

(18) Yuan, X.; Cai, C.; Chen, S.; Chen, S.; Yu, Z.; Balk, S. P. Androgen Receptor Functions in Castration-Resistant Prostate Cancer and Mechanisms of Resistance to New Agents Targeting the Androgen Axis. *Oncogene* **2014**, *33* (22), 2815–2825.

(19) Shore, N. D.; Chowdhury, S.; Villers, A.; Klotz, L.; Robert Siemens, D.; Phung, D.; van Os, S.; Hasabou, N.; Wang, F.; Bhattacharya, S.; Heidenreich, A. Efficacy and Safety of Enzalutamide versus Bicalutamide for Patients with Metastatic Prostate Cancer (TERRAIN): A Randomised, Double-Blind, Phase 2 Study. *Lancet Oncol.* **2016**, *17* (2), 153–163.

(20) Korpal, M.; Korn, J. M.; Gao, X.; Rakiec, D. P.; Ruddy, D. A.; Doshi, S.; Yuan, J.; Kovats, S. G.; Kim, S.; Cooke, V. G.; Monahan, J. E.; Stegmeier, F.; Roberts, T. M.; Sellers, W. R.; Zhou, W.; Zhu, P. An F876l Mutation in Androgen Receptor Confers Genetic and Phenotypic Resistance to MDV3100 (Enzalutamide). *Cancer Discov.* **2013**, *3* (9), 1030–1043.

(21) Joseph, J. D.; Lu, N.; Qian, J.; Sensintaffar, J.; Shao, G.; Brigham, D.; Moon, M.; Maneval, E. C.; Chen, I.; Darimont, B.; Hager, J. H. A Clinically Relevant Androgen Receptor Mutation Confers Resistance to Second-Generation Antiandrogens Enzalutamide and ARN-509. *Cancer Discov.* **2013**, *3* (9), 1020–1029.

(22) Moilanen, A.-M.; Riikonen, R.; Oksala, R.; Ravanti, L.; Aho, E.; Wohlfahrt, G.; Nykänen, P. S.; Törmäkangas, O. P.; Palvimo, J. J.; Kallio, P. J. Discovery of ODM-201, a New-Generation Androgen Receptor Inhibitor Targeting Resistance Mechanisms to Androgen Signaling-Directed Prostate Cancer Therapies. *Sci. Rep.* **2015**, *5* (May), 12007.

(23) Fizazi, K.; Massard, C.; Bono, P.; Jones, R.; Kataja, V.; James, N.; Garcia, J. A.; Protheroe, A.; Tammela, T. L.; Elliott, T.; Mattila, L.; Aspegren, J.; Vuorela, A.; Langmuir, P.; Mustonen, M. Activity and Safety of ODM-201 in Patients with Progressive Metastatic Castration-Resistant Prostate Cancer (ARADES): An Open-Label Phase 1 Dose-Escalation and Randomised Phase 2 Dose Expansion Trial. *Lancet Oncol.* **2014**, *15* (9), 975–985.

(24) Purushottamachar, P.; Kwegyir-Afful, A. K.; Martin, M. S.; Ramamurthy, V. P.; Ramalingam, S.; Njar, V. C. O. Identification of Novel Steroidal Androgen Receptor Degrading Agents Inspired by Galeterone 3β-Imidazole Carbamate. *ACS Med. Chem. Lett.* **2016**, *7* (7), 708–713.

(25) Wang, R.; Lin, W.; Lin, C.; Li, L.; Sun, Y.; Chang, C. ASC-J9® Suppresses Castration Resistant Prostate Cancer Progression via Degrading the Enzalutamide-Induced Androgen Receptor Mutant AR-F876L. *Cancer Lett.* **2016**, *379* (1), 154–160.

(26) Guerrini, A.; Tesei, A.; Ferroni, C.; Paganelli, G.; Zamagni, A.; Carloni, S.; Di Donato, M.; Castoria, G.; Leonetti, C.; Porru, M.; De Cesare, M.; Zaffaroni, N.; Beretta, G. L.; Del Rio, A.; Varchi, G. A New Avenue toward Androgen Receptor Pan-Antagonists: C2 Sterically Hindered Substitution of Hydroxy-Propanamides. *J. Med. Chem.* **2014**, *57* (17), 7263–7279.

(27) Chini, M. G.; Ferroni, C.; Cantone, V.; Dambruoso, P.; Varchi, G.; Pepe, A.; Fischer, K.; Pergola, C.; Werz, O.; Bruno, I.; Riccio, R.; Bifulco, G. Elucidating New Structural Features of

the Triazole Scaffold for the Development of mPGES-1 Inhibitors. *Med. Chem. Commun.* **2014**, *6* (1), 75–79.

(28) Pepe, A.; Pamment, M.; Kim, Y. S.; Lee, S.; Lee, M.-J.; Beebe, K.; Filikov, A.; Neckers, L.; Trepel, J. B.; Malhotra, S. V. Synthesis and Structure–Activity Relationship Studies of Novel Dihydropyridones as Androgen Receptor Modulators. *J. Med. Chem.* **2013**, *56* (21), 8280–8297.

(29) Kim, Y. S.; Kumar, V.; Lee, S.; Iwai, A.; Neckers, L.; Malhotra, S. V.; Trepel, J. B. Methoxychalcone Inhibitors of Androgen Receptor Translocation and Function. *Bioorg. Med. Chem. Lett.* **2012**, *22* (5), 2105–2109.

(30) Lauria, A.; Delisi, R.; Mingoia, F.; Terenzi, A.; Martorana, A.; Barone, G.; Almerico, A. M. 1,2,3-Triazole in Heterocyclic Compounds, Endowed with Biological Activity, through 1,3-Dipolar Cycloadditions. *European J. Org. Chem.* **2014**, *2014* (16), 3289–3306.

(31) Altimari, J. M.; Niranjan, B.; Risbridger, G. P.; Schweiker, S. S.; Lohning, A. E.; Henderson, L. C. Preliminary Investigations into Triazole Derived Androgen Receptor Antagonists. *Bioorg. Med. Chem.* **2014**, *22* (9), 2692–2706.

(32) Agalave, S. G.; Maujan, S. R.; Pore, V. S. Click Chemistry: 1,2,3-Triazoles as Pharmacophores. *Chem. - An Asian J.* **2011**, *6* (10), 2696–2718.

(33) Huisgen, R.; Szeimies, G.; Möbius, L. 1.3-Dipolare Cycloadditionen, XXXII. Kinetik Der Additionen Organischer Azide an CC-Mehrfachbindungen. *Chem. Ber.* **1967**, *100* (8), 2494–2507.

(34) Rostovtsev, V. V; Green, L. G.; Fokin, V. V; Sharpless, K. B. A Stepwise Huisgen Cycloaddition Process: copper(I)-Catalyzed Regioselective "ligation" of Azides and Terminal Alkynes. *Angew. Chem. Int. Ed. Engl.* **2002**, *41* (14), 2596–2599.

(35) Barral, K.; Moorhouse, A. D.; Moses, J. E. Efficient Conversion of Aromatic Amines into Azides: A One-Pot Synthesis of Triazole Linkages. *Org. Lett.* **2007**, *9* (9), 1809–1811.

(36) Gibtner, T.; Hampel, F.; Gisselbrecht, J. P.; Hirsch, A. End-Cap Stabilized Oligoynes: Model Compounds for the Linear Sp Carbon Allotrope Carbyne. *Chem. Eur. J.* **2002**, *8* (2), 408–432.

(37) Kundu, N. G.; Nandi, B. Depropargylation under Palladium-Copper Catalysis: Synthesis of Diaryl Sulfides. *Tetrahedron* **2001**, *57* (27), 5885–5895.

(38) Ilas, J.; Jakopin, Z.; Borstnar, T.; Stegnar, M.; Kikelj, D. 3,4-Dihydro-2H-1,4-Benzoxazine Derivatives Combining Thrombin Inhibitory and Glycoprotein IIb/IIIa Receptor Antagonistic Activity as a Novel Class of Antithrombotic Compounds with Dual Function. *J. Med. Chem.* **2008**, *51* (18), 5617–5629.

(39) Morris, J. C.; Chiche, J.; Grellier, C.; Lopez, M.; Bornaghi, L. F.; Maresca, A.; Supuran, C. T.; Pouysségur, J.; Poulsen, S.-A. Targeting Hypoxic Tumor Cell Viability with Carbohydrate-Based Carbonic Anhydrase IX and XII Inhibitors. *J. Med. Chem.* **2011**, *54* (19), 6905–6918.

(40) Beckmann, H. S. G.; Wittmann, V. One-Pot Procedure for Diazo Transfer and Azide−Alkyne Cycloaddition: Triazole Linkages from Amines. *Org. Lett.* **2007**, *9* (1), 1–4.

(41) Colombo, M.; Bossolo, S.; Aramini, A. Phosphorus Trichloride-Mediated and Microwave-Assisted Synthesis of a Small Collection of Amides Bearing Strong Electron-Withdrawing Group Substituted Anilines. *J. Comb. Chem.* **2009**, *11* (3), 335–337.

(42) Migliaccio, A.; Castoria, G.; Giovannelli, P.; Auricchio, F. Cross Talk between Epidermal Growth Factor (EGF) Receptor and Extra Nuclear Steroid Receptors in Cell Lines. *Mol. Cell. Endocrinol.* **2010**, *327* (1–2), 19–24.

(43) Edwards, J.; Krishna, N. S.; Grigor, K. M.; Bartlett, J. M. S. Androgen Receptor Gene Amplification and Protein Expression in Hormone Refractory Prostate Cancer. *Br. J. Cancer* **2003**, *89* (3), 552–556.

(44) Antonarakis, E. S.; Lu, C.; Wang, H.; Luber, B.; Nakazawa, M.; Roeser, J. C.; Chen, Y.; Mohammad, T. A.; Chen, Y.; Fedor, H. L.; Lotan, T. L.; Zheng, Q.; De Marzo, A. M.; Isaacs, J. T.; Isaacs, W. B.; Nadal, R.; Paller, C. J.; Denmeade, S. R.; Carducci, M. A.; Eisenberger, M. A.; Luo, J. AR-V7 and Resistance to Enzalutamide and Abiraterone in Prostate Cancer. *N. Engl. J. Med.* **2014**, *371* (11), 1028–1038.

(45) Guo, Z.; Yang, X.; Sun, F.; Jiang, R.; Linn, D. E.; Chen, H.; Chen, H.; Kong, X.; Melamed, J.; Tepper, C. G.; Kung, H. J.; Brodie, A. M. H.; Edwards, J.; Qiu, Y. A Novel Androgen Receptor Splice Variant Is up-Regulated during Prostate Cancer Progression and Promotes Androgen Depletion-Resistant Growth. *Cancer Res.* **2009**, *69* (6), 2305–2313.

(46) Baell, J. B.; Gable, R. W.; Harvey, A. J.; Toovey, N.; Herzog, T.; Hänsel, W.; Wulff, H. Khellinone Derivatives as Blockers of the Voltage-Gated Potassium Channel Kv1. 3: Synthesis and Immunosuppressive Activity. *J. Med. Chem.* **2004**, *47* (9), 2326–2336.

(47) Lagorce, D.; Sperandio, O.; Baell, J. B.; Miteva, M. A.; Villoutreix, B. O. FAF-Drugs3: A Web Server for Compound Property Calculation and Chemical Library Design. *Nucleic Acids Res.* **2015**, *43* (W1), W200–W207.

(48) Bohl, C. E.; Gao, W.; Miller, D. D.; Bell, C. E.; Dalton, J. T. Structural Basis for Antagonism and Resistance of Bicalutamide in Prostate Cancer. *Proc. Natl. Acad. Sci. U. S. A.* **2005**, *102* (17), 6201–6206.

(49) Tesei, A.; Leonetti, C.; Di Donato, M.; Gabucci, E.; Porru, M.; Varchi, G.; Guerrini, A.; Amadori, D.; Arienti, C.; Pignatta, S.; Paganelli, G.; Caraglia, M.; Castoria, G.; Zoli, W. Effect of Small Molecules Modulating Androgen Receptor (SARMs) in Human Prostate Cancer Models. *PLoS One* **2013**, *8* (5), 1–12.

(50) Skehan, P.; Storeng, R.; Scudiero, D.; Monks, A.; McMahon, J.; Vistica, D.; Warren, J. T.; Bokesch, H.; Kenney, S.; Boyd, M. R. New Colorimetric Cytotoxicity Assay for Anticancer-Drug Screening. *JNCI J. Natl. Cancer Inst.* **1990**, *82* (13), 1107–1112.

(51) Monks, A.; Scudiero, D.; Skehan, P.; Shoemaker, R.; Paull, K.; Vistica, D.; Hose, C.; Langley, J.; Cronise, P.; Vaigro-Wolff, A.; Gray-Goodrich, M.; Campbell, H.; Mayo, J.; Boyd, M. Feasibility of a High-Flux Anticancer Drug Screen Using a Diverse Panel of Cultured Human Tumor Cell Lines. *JNCI J. Natl. Cancer Inst.* **1991**, *83* (11), 757–766.

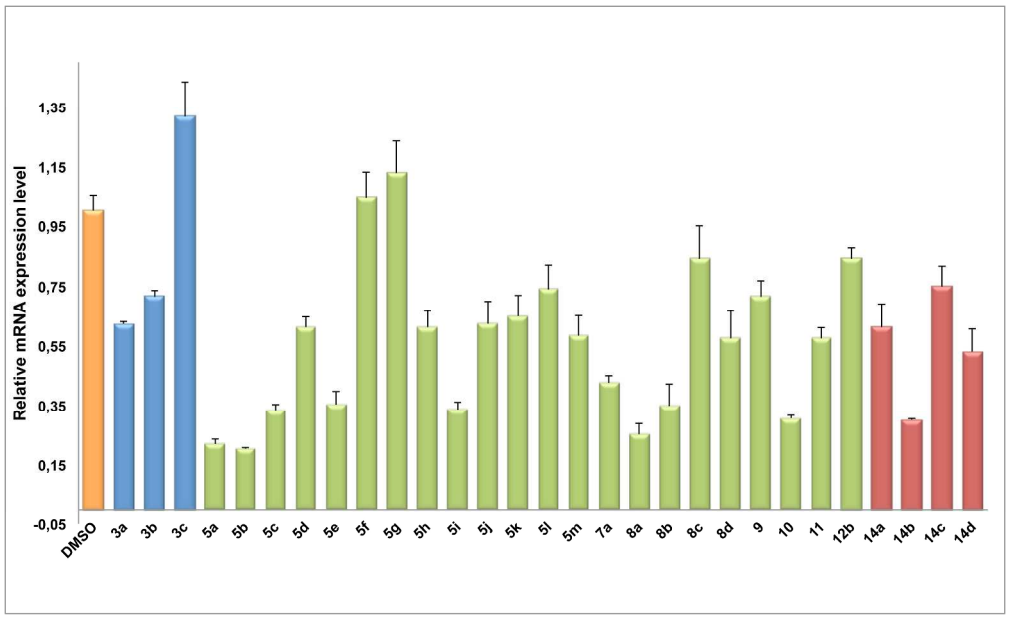

Evaluation of PSA mRNA levels after exposure of LNCaP cell lines to triazoles. Twenty-four hours after seeding, cells were treated for 24 h with 10 μM compounds. Cells were then collected, processed for mRNA extraction and analyzed using RT-qPCR. Blue bars: no-spacer triazoles (type I); Green bars: one-spacer triazoles (type II); Red bars two-spacer triazoles (type III)

292x178mm (300 x 300 DPI)

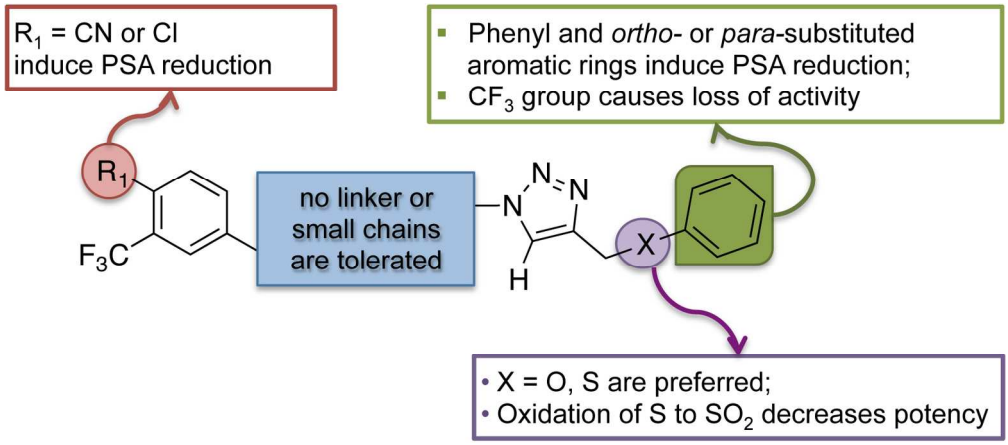

Influence of 1,4-triazole ring substituents on the PSA level reduction

156x68mm (300 x 300 DPI)

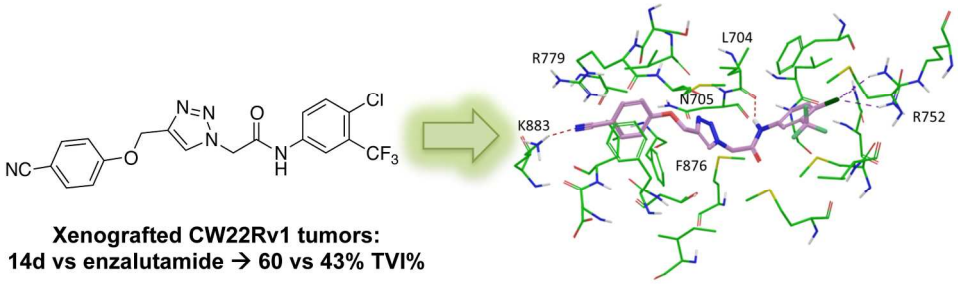

Graphical abstract

190x54mm (300 x 300 DPI)

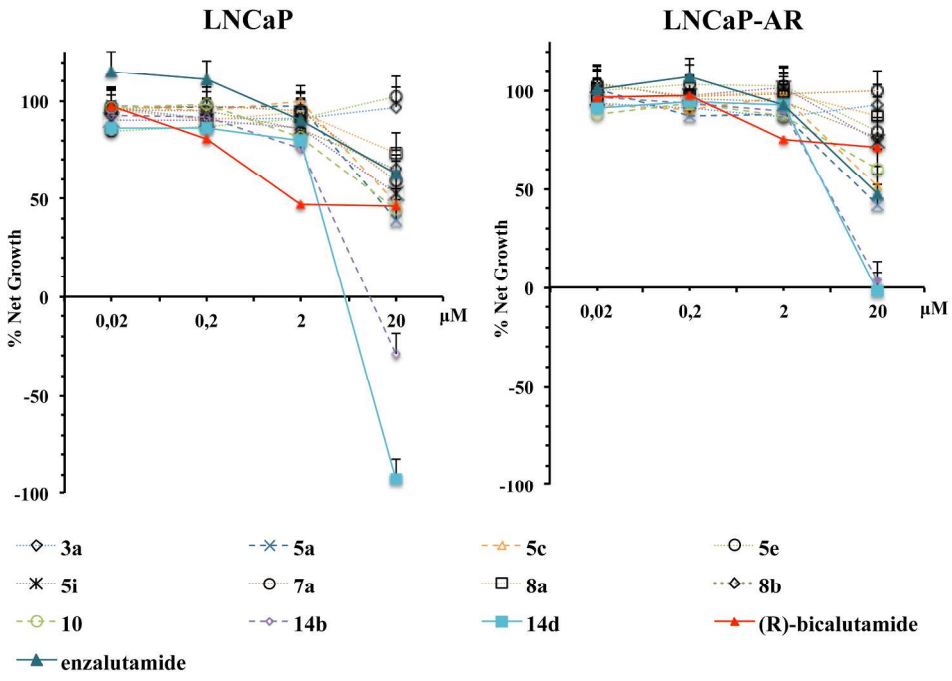

Cytotoxic activity of novel triazole derivatives against human PC LNCaP (A) and LNCaP-AR (B) cells. Twenty-four hours after seeding, cells were exposed to the compounds for 144 h to the compounds and cytotoxicity was measured using a sulforhodamine B (SRB) assay. (R)-bicalutamide and enzalutamide were used as references. The mean of three independent experiments is reported

225x160mm (300 x 300 DPI)

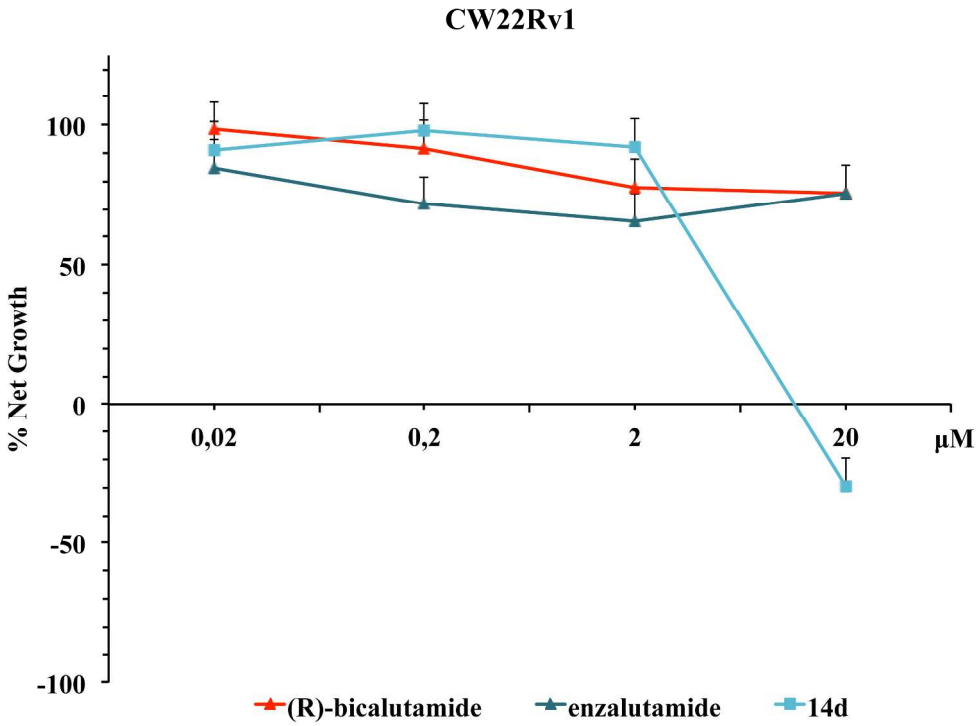

Cytotoxic activity of 14d against human CW22Rv1 cells. Twenty-four hours after seeding, cells were exposed for 144 h to the compounds. The cytotoxic potency was measured using a sulforhodamine B (SRB) assay. (R)-bicalutamide and enzalutamide were used as references. The mean of three independent experiments is reported

237x178mm (300 x 300 DPI)

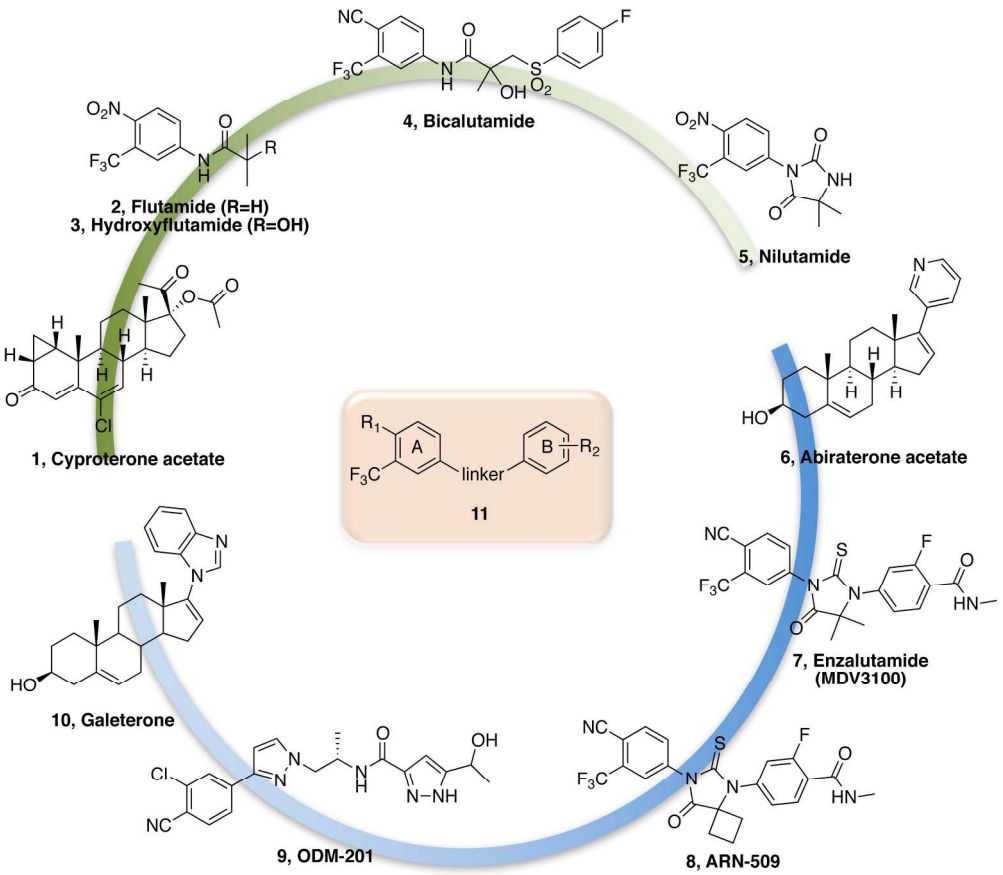

Figure 1. Androgen receptor targeting therapeutics for the treatment of PC.

197x171mm (300 x 300 DPI)

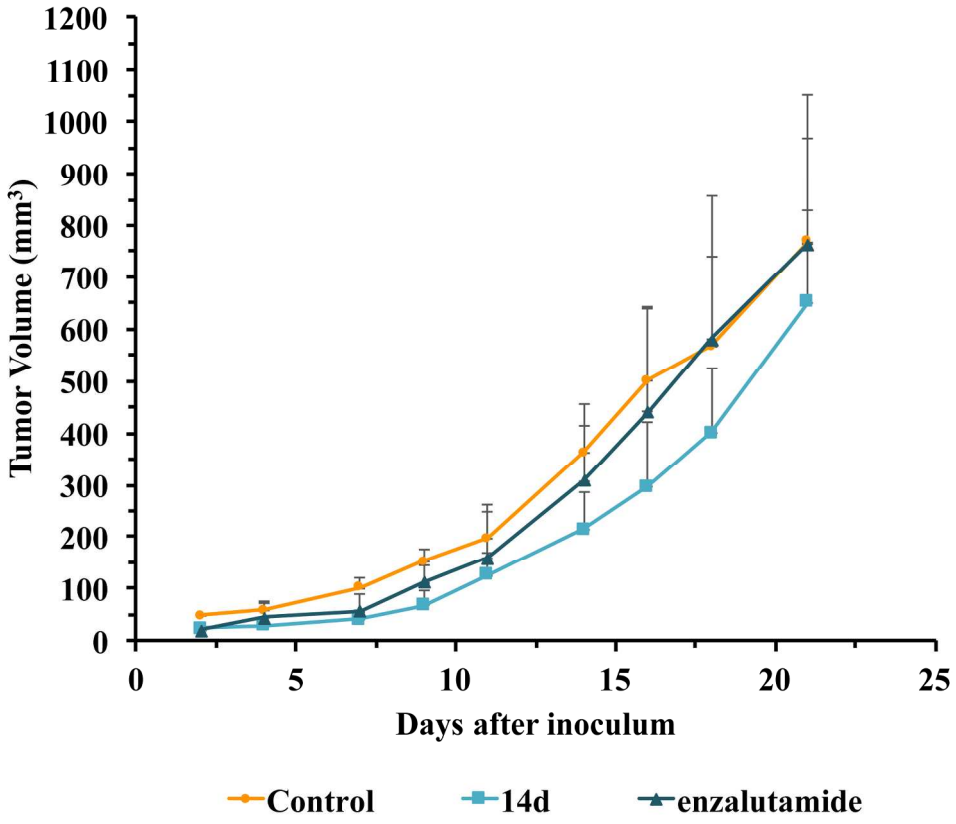

Antitumor activity of oral 14d and enzalutamide against human prostate CW22Rv1 carcinoma tumor xenograft. CW22Rv1 cells (5x106/mouse) were injected into the right flank of the mice on day 0. Treatment started when tumors were not palpable (day 1). Drugs or vehicle (for Control group), were administrated orally at the dose of 50mg/kg according the qdx5/wx3w schedule. Tumor size was measured by caliper, and tumor volume calculated using: TV= a × b2/2, where a and b are the long and short diameters of the tumor, respectively. Points, mean from five mice per group; bars, SD.

196x168mm (300 x 300 DPI)

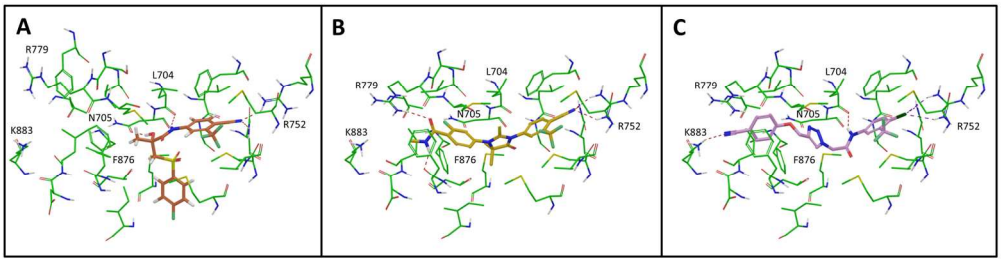

Figure 8. Putative binding mode of AR modulators. Predicted binding mode of (R)-bicalutamide (A), enzalutamide (B) and compound 14d (C). Hydrogen bonds are represented as red dotted lines. Binding pose of (R)-bicalutamide was obtained through rigid docking starting from AR crystallographic structures (pdb code 2AXA), whereas poses of enzalutamide and 14d were obtained from IFD simulations.

177x47mm (300 x 300 DPI)